

**Decoupled Electrochemical Water-Splitting Systems: A
Review and Prospective**

Journal:	<i>Energy & Environmental Science</i>
Manuscript ID	EE-REV-04-2021-001226.R1
Article Type:	Review Article
Date Submitted by the Author:	07-Jun-2021
Complete List of Authors:	Ifkovits, Zachary; California Institute of Technology, Division of Chemistry and Chemical Engineering Evans, Jake; California Institute of Technology Meier, Madeline; California Institute of Technology, Chemistry and Chemical Engineering Papadantonakis, Kimberly; California Institute of Technology, Chemistry and Chemical Engineering Lewis, Nathan S.; California Institute of Technology, Chemistry and Chemical Engineering

Decoupled Electrochemical Water-Splitting Systems: A Review and Prospective

Broader Context:

Water electrolyzers paired with electricity generated from renewable resources can provide green hydrogen, i.e. hydrogen formed with no associated carbon dioxide emissions. Conventional electrolysis proceeds by submerging two charged electrodes into an aqueous environment, simultaneously generating hydrogen at one electrode and oxygen at the other. The tight spatial and temporal coupling of the hydrogen and oxygen can cause issues associated with safety, longevity of device components, and system flexibility. Decoupled electrolysis separates the hydrogen and oxygen evolution reactions by alternately pairing them to the oxidation or reduction of an intermediate compound, known as a mediator. The physical implementation and operation of the system varies substantially depending on the choice of mediator, of which potentially hundreds exist. Decoupled electrolysis systems can by nature be intrinsically safe, modular, and flexible, making them an interesting technology for a sustainable energy future. Research in this field combines important concepts from electrolysis, batteries, reactor design, redox flow batteries, and photovoltaics, as well as other disciplines. Herein, we summarize the progress of this fast-growing field, evaluate the proposed benefits of decoupled electrolysis systems, and discuss some of the technological and economic hurdles that remain.

Decoupled Electrochemical Water-Splitting Systems: A Review and Prospective

Zachary P. Ifkovits,¹ Jake M. Evans,¹ Madeline C. Meier,¹ Kimberly M. Papadantonakis,¹ and Nathan S. Lewis^{1,2*}

¹Division of Chemistry and Chemical Engineering, California Institute of Technology, Pasadena, California 91125, USA.

²Beckman Institute Molecular Materials Resource Center, California Institute of Technology, Pasadena, California 91125, USA.

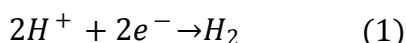
*Corresponding author: nslewis@caltech.edu

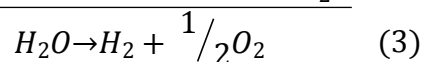
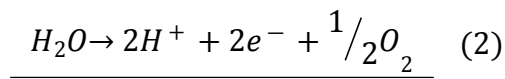
Summary:

Electrochemical water splitting is a promising technology to renewably generate hydrogen fuel from water. One particular drawback of conventional water splitting is that the hydrogen-forming reduction reaction is tightly coupled, both spatially and temporally, to the oxygen-forming oxidation reaction. This coupling poses challenges in both conventional and direct-solar-powered electrolysis systems, including gas crossover, separator degradation, and sometimes necessitating the use of precious metal catalysts. In decoupled water splitting, the conventional electrolysis reactions are separated spatially, temporally, or both, via coupling to an intermediate redox mediator. Decoupled water-splitting systems are flexible and modular by nature, with other proposed benefits including facile coupling to renewable power sources, utilization of earth-abundant catalysts, and intrinsically safe operation. Here we review recent advances in decoupled water splitting and related fields, mainly categorizing decoupled systems by mediator phase and standard potential. We offer insight to how decoupling may be advantageous, and which tradeoffs need to be considered for practical implementation. We conclude our review with discussion of known technological hurdles and note opportunities for future discovery.

Introduction:

Renewably generated hydrogen is being pursued as a carbon-neutral fuel for use in combustion, engines, turbines and fuel cells.¹ Renewable hydrogen can be generated through the electrolysis of water – also known as electrochemical water splitting – driven by electricity generated using renewable resources. In low-temperature electrochemical water splitting, two electrodes are placed in contact with an aqueous electrolyte, and a voltage sufficient to cause water to split into its elemental components, hydrogen (H₂) and oxygen (O₂), is applied across the electrodes. The overall water-splitting reaction is the sum of a reduction half-reaction and an oxidation half-reaction that occur at the cathode and anode, respectively. Equation 1 shows the water-reduction half-reaction, frequently called the hydrogen-evolution reaction (HER), in an acidic electrolyte. Equation 2 shows the water-oxidation half-reaction, frequently called the oxygen-evolution reaction (OER), also for an acidic electrolyte. Equation 3 shows the net reaction of Eq. 1 and Eq. 2, which is the overall water-splitting reaction.





The electrons travel in an external circuit from the anode to the cathode, while protons migrate through solution from the anode to the cathode, maintaining charge neutrality. Similar reactions exist for water splitting in alkaline environments, where hydroxide is the relevant ion instead of protons. A schematic of a water-splitting cell is shown in **Figure 1**.

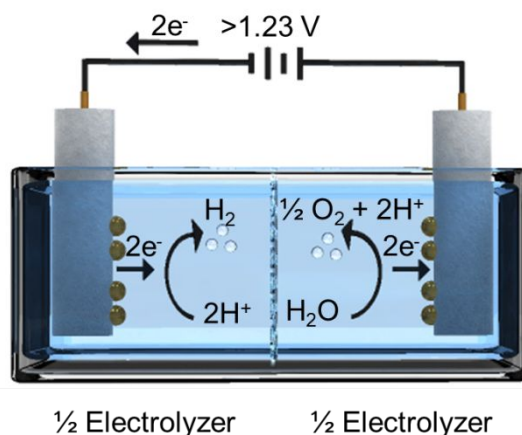
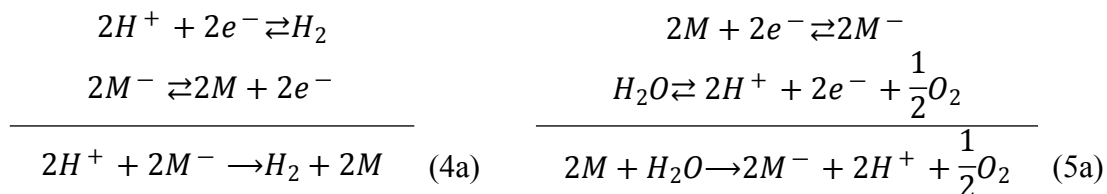


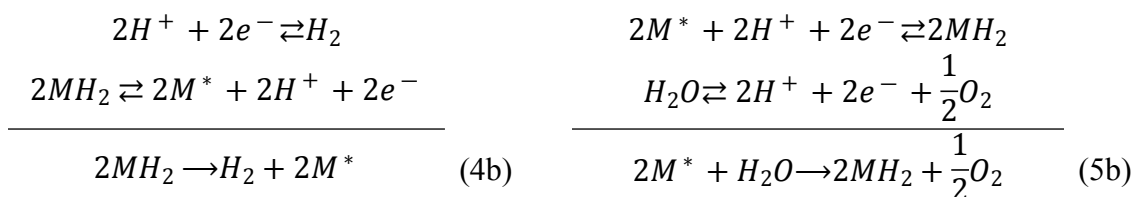
Figure 1. Schematic of a water-splitting cell, showing a cathode (left) and an anode (right) separated by a gas-impermeable ion-exchange membrane (middle). The brown circles represent catalysts for either water reduction (cathode) or water oxidation (anode).

By definition, in water splitting the generation of H_2 and O_2 are coupled directly, meaning that H_2 and O_2 are produced simultaneously at the same current and in a strictly defined stoichiometric ratio of 2:1. To avoid generating an explosive mixture of $H_2(g)$ and $O_2(g)$ during electrochemical water splitting, the anode and cathode are separated by an ion-exchange membrane or by an ion-permeable separator, such as ceramic or metal-oxide diaphragms.² Given the thermodynamics of water splitting (1.23 V at 25 °C and 1 atm), and current-density-dependent losses due to catalytic overpotentials and cell resistance, in practice electrochemical water splitting at 25 °C generally requires ≥ 1.7 V. A state-of-the-art polymer-electrolyte-membrane (PEM) electrolyzer operating at 80 °C requires 1.7 V, and has a total catalytic overpotential of approximately 500 mV at a current density of 1.0 A/cm².² Minimizing the catalytic overpotentials often requires the use of precious metal catalysts.

Decoupled electrochemical water splitting recently has become a prominent topic in electrochemistry due to its potential to provide a flexible alternative to conventional electrolytic water splitting for the generation of hydrogen.³⁻⁹ In decoupled electrochemical water splitting, the HER is coupled to an oxidation half-reaction of a redox mediator (M^{\cdot}), while the OER is coupled to a reduction half-reaction of M :



The net reaction (sum of Eq. 4a and Eq. 5a) is equivalent to the water-splitting reaction (Eq. 3), and H_2 and O_2 are collected as outputs. The mediator is cycled back and forth through oxidation states in a manner akin to either a redox-flow battery (RFB) or a solid-state battery, depending on whether the mediator is in a liquid or solid phase. In both electrochemical water splitting and decoupled electrochemical water splitting, the only system inputs are water and electrical power, and the only outputs are H_2 and O_2 . As written, Eq. 4a and Eq. 5a are not individually in proton balance, meaning that the pH will change if Eq. 4a is operated without Eq. 5a (and vice-versa). However, since pH is on a log scale and can be determined largely by the electrolyte, the actual pH change during independent operation of the decoupled cells depends on both the initial pH of the electrolyte and the current passed during decoupled operation. Eq. 4a and Eq. 5a can be modified slightly for mediators that also uptake and release protons during operation:



The net reaction is still equivalent to the water-splitting reaction (Eq. 3), but the system remains in proton balance. Mediators operated in alkaline environments undergo similar reactions as those shown in Eq. 4 and Eq. 5, but are balanced with hydroxide ions rather than protons.

Coupling to M allows separation of the HER and OER in time, space, or both. Purported benefits of such arrangements include: (1) the removal or substitution of costly electrolyzer components, such as ion-exchange membranes and precious metal catalysts; (2) facile coupling with intermittent renewable energy sources; (3) membrane-free generation of pressurized

hydrogen; and, (4) mitigation of the risk of explosion that accompanies simultaneous production of H_2 and O_2 during water splitting. These and other benefits are discussed further in the “Discussion and Prospective” section of this report.

M can be either a soluble redox couple, such as V^{3+}/V^{2+} or $[Fe(CN)_6]^{3-/4-}$, or a solid, such as $NiOOH/Ni(OH)_2$.¹⁰ The phase of M affects the physical components as well as the operation of the system. Systems with a soluble redox mediator can operate under either static or flow conditions, because M can be pumped between chambers. In systems with solid-state mediators, M typically is integrated with an electrode that can be moved between cells to be partnered with the HER or OER.

Depending on the choice of M, the standard potential $E^0(M^{0/-})$ may fall either inside or outside of the potential range bracketed by $E^0(H^+/H_2)$ and $E^0(O_2/H_2O)$. Notional current-voltage data for these two situations are shown in **Figure 2**. The position of $E^0(M^{0/-})$ relative to $E^0(H^+/H_2)$ and $E^0(O_2/H_2O)$ affects how the system is configured physically in addition to how it operates in practice. If $E^0(M^{0/-})$ falls between $E^0(H^+/H_2)$ and $E^0(O_2/H_2O)$, then coupling to M can reduce the maximum instantaneous power required by the system by dividing the thermodynamically required voltage for water splitting into multiple non-spontaneous steps (see **Figure 2a**). If $E^0(M^{0/-})$ falls outside of the range from $E^0(H^+/H_2)$ to $E^0(O_2/H_2O)$, then coupling to M can increase the thermodynamically required voltage for the first step, but the second step can proceed spontaneously without any external circuit or electrochemical cell (see **Figure 2b**).

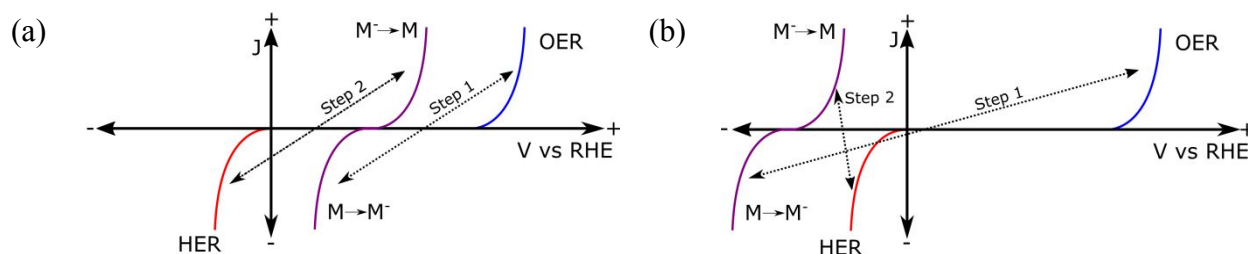


Figure 2. Notional current-voltage behavior for decoupled water-splitting systems. (a) $E^0(M^{0/-})$ falls between $E^0(H^+/H_2)$ and $E^0(O_2/H_2O)$, dividing the thermodynamically required voltage for water splitting into two non-spontaneous steps. (b) $E^0(M^{0/-})$ falls outside of the range from $E^0(H^+/H_2)$ to $E^0(O_2/H_2O)$. In this case, the voltage required for step 1 is greater than that required for water splitting, but step 2 proceeds spontaneously.

Decoupled electrochemical water-splitting systems therefore can be sorted into four classes, based on the phase of M and whether one or both steps require input power (**Figure 3**).

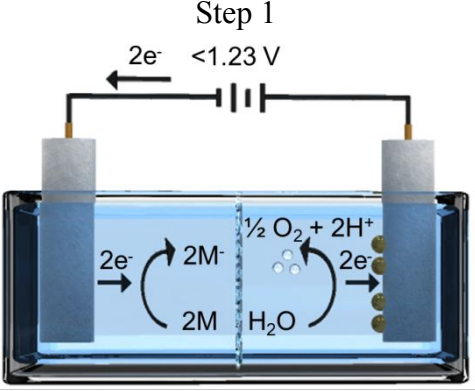
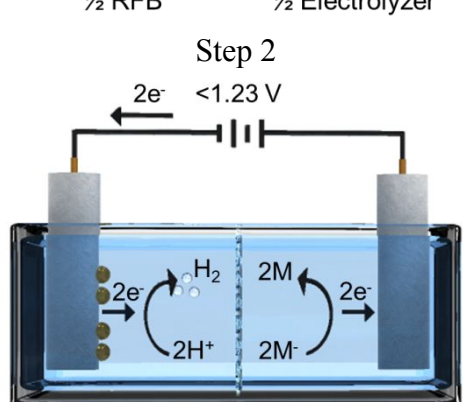
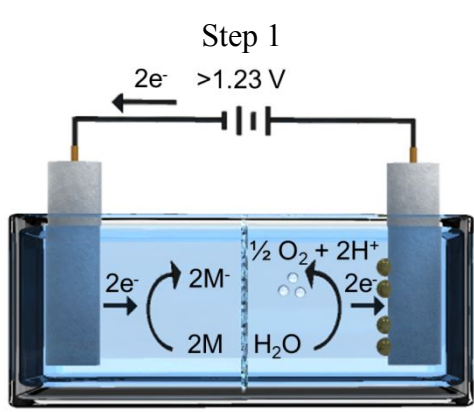
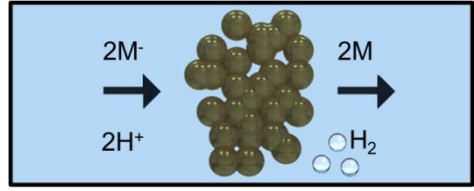
For liquid-mediated systems with two non-spontaneous steps (Type 1), the cell for each of the two steps is composed of an RFB half-cell and an electrolysis half-cell. The electrolyte containing the mediator that was reduced in Step 1 can be pumped to a second cell where the mediator is re-oxidized; alternatively, the electrode for the electrolysis half-cell could be exchanged and the cell could be run with polarity opposite to that used in Step 1. Liquid-mediated systems require a separator to keep the mediator and electrolysis products contained within their proper half-cells.

Liquid-mediated systems with a spontaneous second step (Type 2) generally resemble a cell composed of an RFB half-cell and an electrolysis half-cell, paired with a catalyst bed. Systems of this type do not require the HER to occur over an electrode surface, because external power input is not required to drive that step.

Solid-mediated systems with two non-spontaneous steps (Type 3) typically use a single decoupling electrode that is paired alternately with the proper electrode for either the HER or OER. In general, the cell for each of the two steps in these systems is composed of an electrolysis half-cell and a battery half-cell.

Solid-mediated systems with a spontaneous second step (Type 4) generally are configured similarly to their non-spontaneous counterparts. Specifically, the cell for each of the two steps is composed of an electrolysis half-cell and a battery half-cell; however, the second cell does not require an external power source.

All four types of decoupled electrolysis systems allow some components, such as electrodes and cells, to be shared among Step 1 and Step 2.

Phase of M	Two Non-Spontaneous Steps	One Spontaneous Step and One Non-Spontaneous Step
Liquid	<p style="text-align: center;">Step 1</p>  <p style="text-align: center;">Step 2</p> 	<p style="text-align: center;">Step 1</p>  <p style="text-align: center;">Step 2</p> 

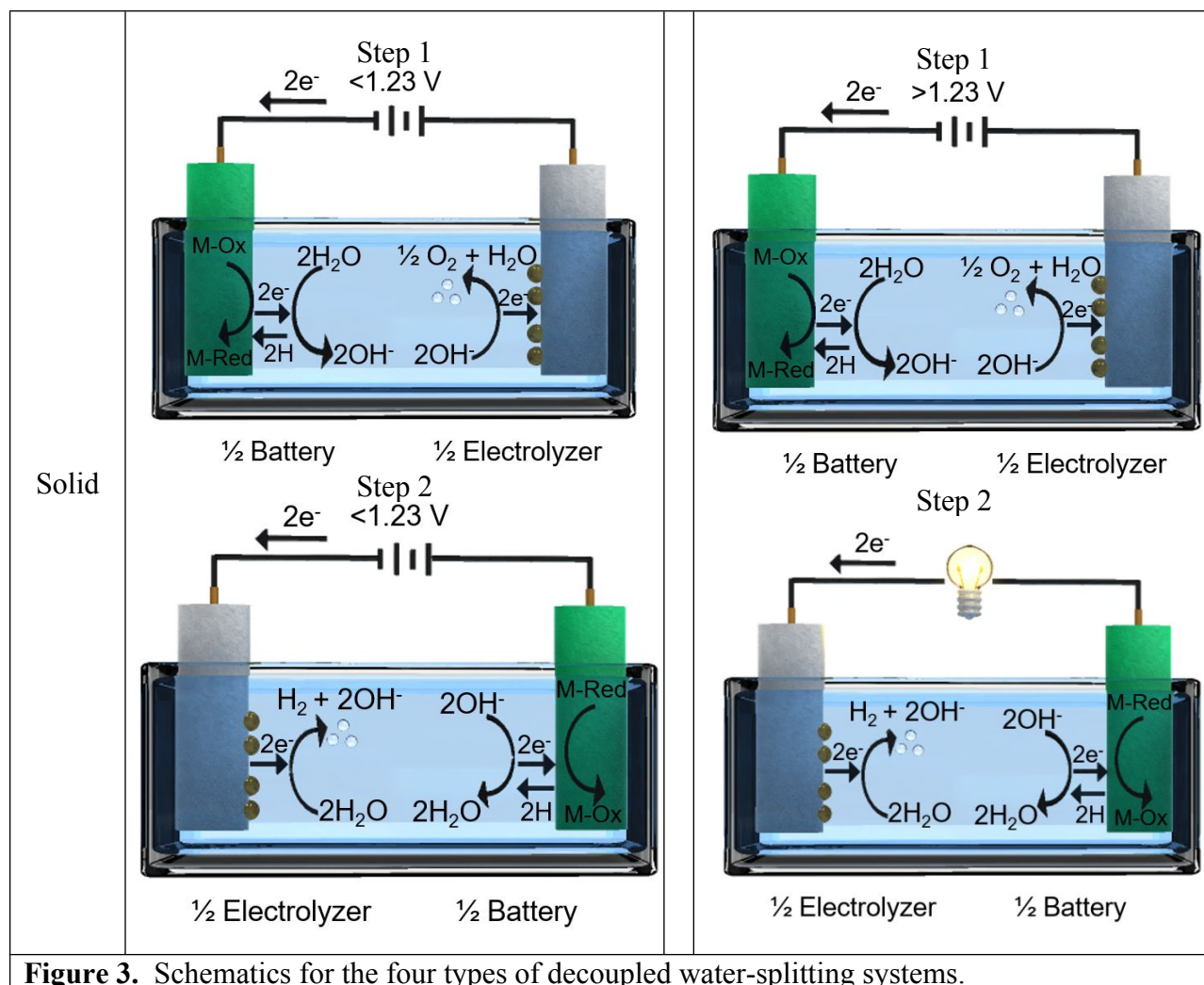


Figure 3. Schematics for the four types of decoupled water-splitting systems.

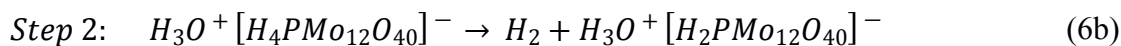
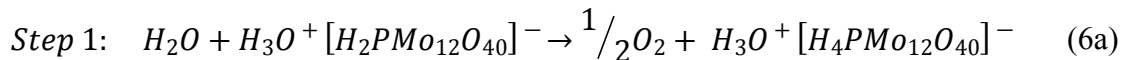
Examples of Decoupled Electrochemical Water-Splitting Systems

Table 1 lists the properties of mediators commonly used in decoupled water-splitting systems that use soluble mediators (Type 1 and Type 2 systems).

Type 1: Liquid Mediator, Two Non-Spontaneous Steps

In 2013, Symes and Cronin reported a Type 1 system with phosphomolybdic acid (PMA) as a polyoxometalate (POM) mediator in acidic media.¹¹ The PMA was an electron-coupled-proton buffer (ECPB), in which the uptake of electrons by PMA was coupled with the uptake of protons, thereby maintaining proton balance during operation. In the first step, the generation of oxygen over the anode was paired with the reduction of PMA (Eq. 6a). When the mediator was

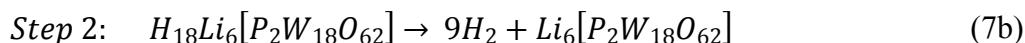
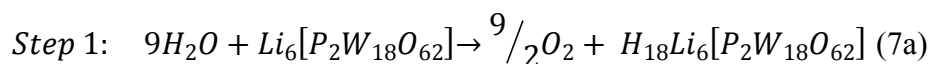
fully reduced, the polarity of the externally applied voltage was reversed, leading to the generation of hydrogen and the oxidation of PMA (Eq. 6b).¹¹



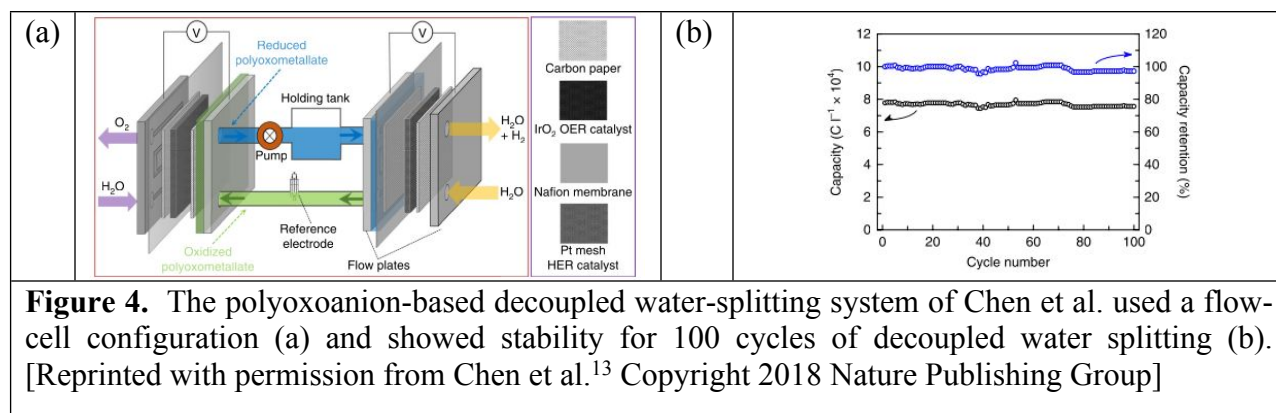
Since H₂ and O₂ were not generated simultaneously, an inexpensive benzoylated cellulose membrane, that was freely permeable to H₂, was also used to keep the PMA isolated in its proper half-cell. The benzoylated cellulose membrane had similar performance to the Nafion membrane used for most of the study.

Recently, PMA was utilized by Wu et al. in a decoupled electrolysis system with a bipolar membrane, allowing for alkaline electrolysis with an acidic mediator.¹² In their system, the PMA redox half-reactions were paired with electrolysis half-reactions in a 0.5-1.5 M NaOH solution. As earth-abundant catalysts – especially OER catalysts – exhibit improved activity and stability in base compared to acid, the mediated bipolar membrane system allowed low-overpotential nickel-based electrodes to be used for 20 h of stable cycling.

Chen et al. then modified the ECPB for increased energy density.¹³ Previously reported inorganic ECPB systems could uptake two electrons and two protons, whereas the highly reducible Li₆[P₂W₁₈O₆₂] polyoxoanion-based ECPB system could reversibly uptake a maximum of 18 electrons and 18 protons (Eq. 7).

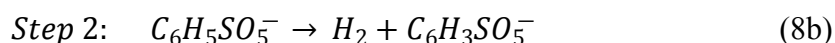
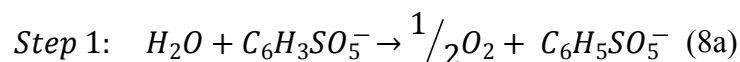


The polyoxoanion-based ECPB exhibited reversible redox activity at potentials both positive and negative of the potential of the reversible hydrogen electrode (RHE), allowing some of the reduced ECPB to be used for a spontaneous hydrogen-evolution step (Type 2). However, accessing the full energy-storage capacity of the mediator required power input in both steps. This system used a flow-cell configuration as shown in **Figure 4a**, which is typical of other flow-cell designs for decoupled water splitting. Experiments showed retention of ~ 100% of the capacity of the mediator after 100 decoupled cycles, shown in **Figure 4b**.

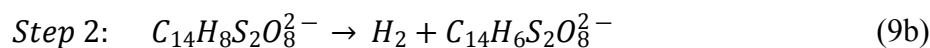
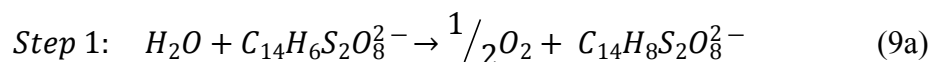


Given the higher electron- and proton-uptake capacity of the polyoxoanion-based ECPB mediator compared to previous ECPBs, the species can be viewed as an energy-storage or hydrogen-storage medium. At the solubility limit of 1.9 M, this redox mediator would have a hydrogen-storage capacity of 34.2 g H₂/L, about half that of cryogenic H₂ (71 g H₂/L).¹⁴

Smaller organic mediators have been utilized in Type 1 systems to replace large inorganic POMs. Rausch et al. showed that hydroquinone sulfonate (HQS) is a suitable mediator for decoupled water splitting (Eq. 8).¹⁵



HQS differs from POMs in that its molecular weight is an order of magnitude lower than POMs, and the elements that comprise HQS are more abundant than the metals in POMs. The decreased molecular weight reduces the mass of mediator required to achieve a given energy density and improves solution-transport properties, but leads to increased permeation of the mediator through the membrane separator. The HQS degraded by ~ 1% per cycle over 20 cycles, as quantified by a decrease in charge capacity. Kirkaldy et al. subsequently demonstrated the use of anthraquinone-2,7-disulfonic acid (AQDS) in these systems (Eq. 9).¹⁶

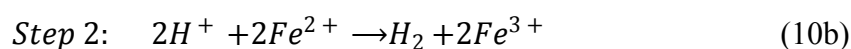
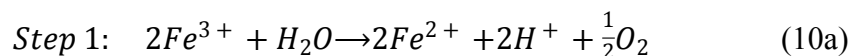


AQDS is similar to HQS but only degraded by 0.06% per cycle over 100 cycles.

In a later report, Cronin's group integrated their Type 1 PMA with a WO₃-FTO photoanode.¹⁷ The photoanode provided the power required to run the first step of the decoupled electrolysis process, specifically the OER and reduction of PMA. With no applied external bias,

this system operated at $\sim 1.2 \text{ mA/cm}^2$, with stable performance on the order of minutes. This system is still classified as “non-spontaneous” because both steps required power input, even though the power input for the first step was produced by illumination of a photoanode.

Both Li et al. and Zhao et al. reported the use of bismuth vanadate crystals to photocatalytically oxidize water and reduce the redox mediators used in their reported systems.¹⁸⁻¹⁹ Li et al. used dispersed BiVO_4 powder as a photocatalyst for the OER in conjunction with reduction of PMA.¹⁸ Zhao et al. used BiVO_4 to oxidize water and reduce Fe(III) to Fe(II) in a “hydrogen farm” (Eq. 10).¹⁹



The reduced iron could then be shuttled inside for its oxidation in conjunction with hydrogen generation. A schematic of the “hydrogen farm” is shown in **Figure 5**.

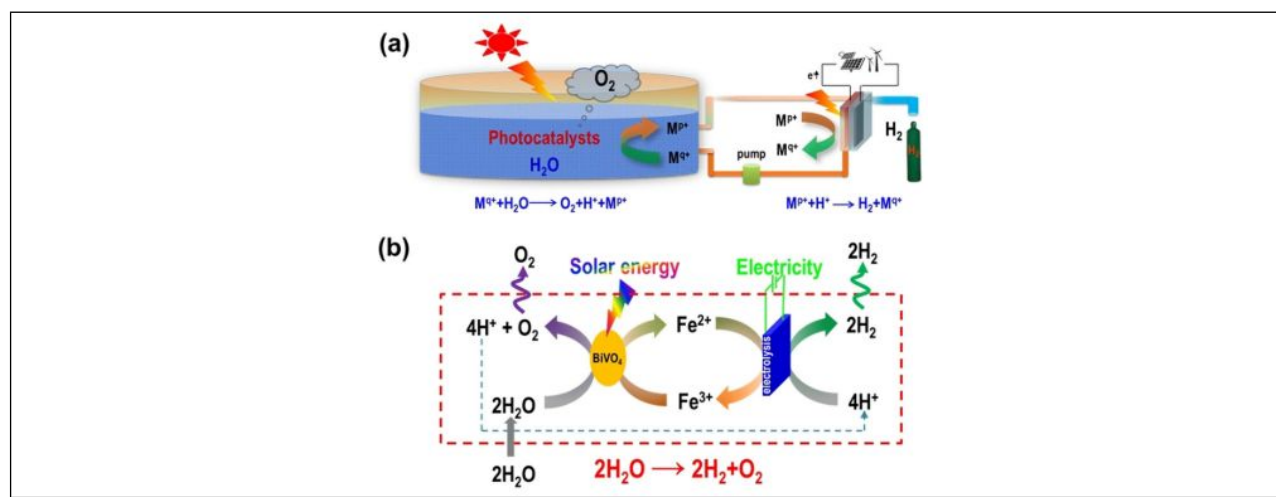
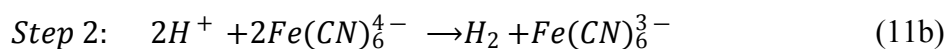
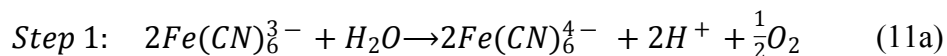


Figure 5. (a) A schematic of a “hydrogen farm” that uses photocatalysts to oxidize water and reduce a liquid-phase mediator. The electrolyte containing the reduced mediator is pumped to another location where it is reoxidized in conjunction with hydrogen evolution. (b) A schematic of an implementation of a hydrogen farm that uses BiVO_4 as a photocatalyst and $\text{Fe}^{3+/2+}$ as a mediator. [Reprinted with permission from Zhao et al.¹⁹ Copyright 2020 Wiley-VCH Verlag GmbH & Co. KGaA]

The hydrogen-farm study focused on engineering the exposed crystal facets of the BiVO_4 to selectively perform both the OER and Fe^{3+} reduction without deleteriously oxidizing Fe^{2+} back to Fe^{3+} . Zhao et al. found that the reoxidation of Fe^{2+} to Fe^{3+} could be prevented by controlling the exposed facets of the BiVO_4 crystals. To explain this result, they hypothesized that 1) photogenerated electrons preferentially accumulate on the (010) facets of the BiVO_4 , whereas

photogenerated holes preferentially accumulate on the (110) facets, and 2) due to the accumulation of positive charge on the (110) facets, electrostatics disfavors the approach of cations such as Fe^{2+} to the electron-accepting facet of BiVO_4 , allowing the amount of reduced Fe to match the maximum theoretical value. To test this hypothesis, the $\text{Fe}^{3+/2+}$ couple was replaced by $[\text{Fe}(\text{CN})_6]^{3-/4-}$, a negatively charged complex anion with a standard potential similar to $\text{Fe}^{3+/2+}$. The net conversion of $[\text{Fe}(\text{CN})_6]^{4-}$ to $[\text{Fe}(\text{CN})_6]^{3-}$ was only approximately 50% of the maximum theoretical value, supporting the hypothesis that – unlike the Fe^{2+} cation – the negatively charged $[\text{Fe}(\text{CN})_6]^{3-}$ was not repelled by the positively charged (110) facets.

Other redox couples commonly used in electrochemistry have been used as mediators for decoupled electrochemical water splitting. Goodwin et al. used potassium $[\text{Fe}(\text{CN})_6]^{3-/4-}$ as an electron reservoir (Eq. 11).²⁰



In this system, the HER and OER were isolated spatially but not temporally. Here, the OER was coupled with the reduction of $[\text{Fe}(\text{CN})_6]^{3-}$ to $[\text{Fe}(\text{CN})_6]^{4-}$, whereas the HER was coupled with the oxidation of $[\text{Fe}(\text{CN})_6]^{4-}$ to $[\text{Fe}(\text{CN})_6]^{3-}$. The application of sufficient voltage (2.0 – 2.6 V) drove the entire system, simultaneously generating pure hydrogen and pure oxygen gases at different locations. The polarization could then be reversed to return the system to its initial state.

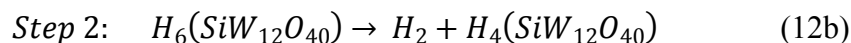
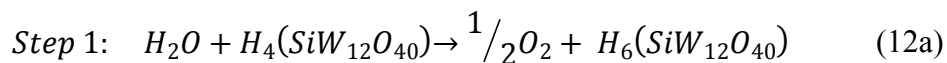
Other researchers have used $[\text{Fe}(\text{CN})_6]^{3-/4-}$ as an electron reservoir for decoupled electrolysis reactions that reduce water to yield H_2 , but yield oxidized organic molecules rather than O_2 . Ma et al. reported the use of $[\text{Fe}(\text{CN})_6]^{3-/4-}$ as an electron reservoir to pair the HER with wastewater treatment in a decoupled manner.²¹ In this system, decontamination was quantified by monitoring the concentration of phenol and the chemical oxygen demand of the anolyte during decoupled electrolysis. At current densities of 16 mA/cm^2 , removal of phenol reached 96.44%. Hydrogen was recovered at faradaic efficiencies in the range of 71.77-99.88%.

Similarly, Sun et al. have paired the HER with the oxidative valorization of 5-hydroxymethylfurfural (HMF) to 2,5-furandicarboxylic acid in a traditional electrolytic cell,²² and have shown that the valorization method can be mediated by $[\text{Fe}(\text{CN})_6]^{3-/4-}$.²³ In the decoupled system, the HER is paired with the oxidation of $[\text{Fe}(\text{CN})_6]^{4-}$ to $[\text{Fe}(\text{CN})_6]^{3-}$, whereas the reduction of $[\text{Fe}(\text{CN})_6]^{3-}$ is paired with the organic upgrading of HMF, all under alkaline conditions. In the same report, Sun et al. utilized (ferrocenylmethyl)trimethylammonium chloride

(FcNCl) as a mediator for decoupled electrolysis in neutral pH. The FcNCl-mediated cell was later powered entirely by a commercial PV cell. In all of the systems mediated by FcNCl or $[\text{Fe}(\text{CN})_6]^{3-/4-}$ as electron reservoirs, proton balance is not maintained during each step. The pH of the electrolyte reproducibly changed from 6.5 to 9, then back to 6.5 as the polarization was reversed during operation of an unbuffered system mediated by FcNCl.

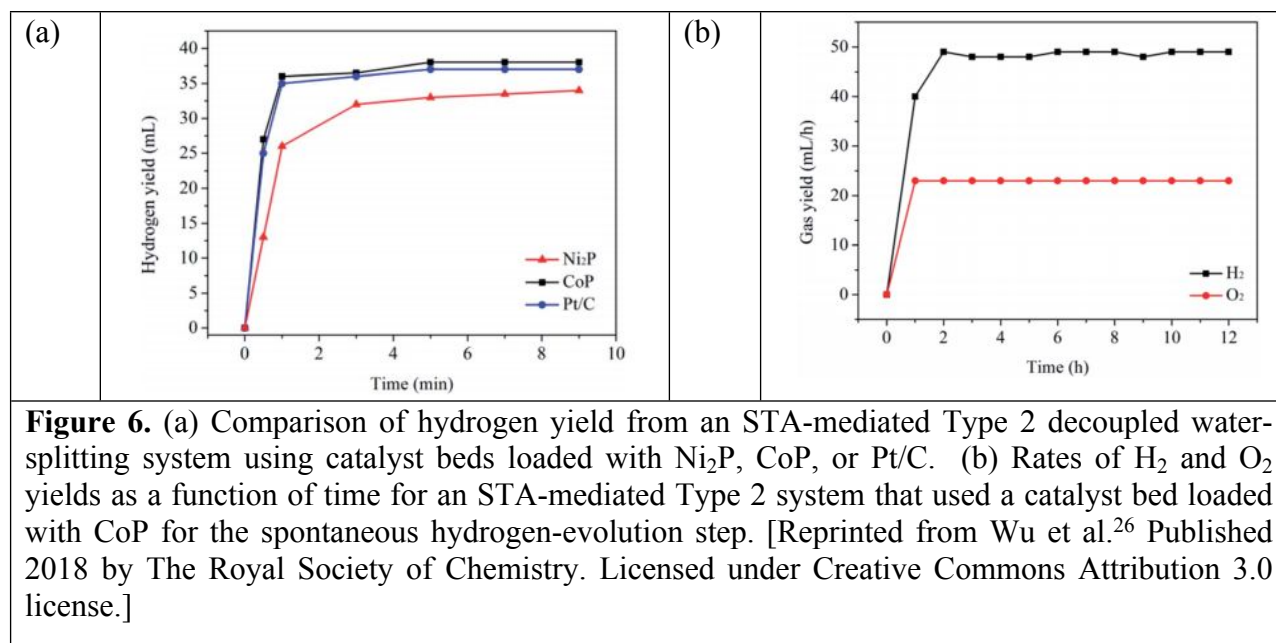
Type 2: Liquid Mediator, Spontaneous

Cronin's group reported a Type 2 system in 2014.²⁴ Similar to their earlier work with PMA,¹¹ the OER was paired with the reduction of silicotungstic acid (STA) (Eq. 12).



Unlike PMA, STA has a reversible redox peak at potentials negative of RHE. When the reduced STA comes in contact with powdered precious metal catalysts, hydrogen gas is released spontaneously. Compared to conventional PEM electrolysis systems that use precious metal electrodes to generate hydrogen at mass-normalized H_2 -production rates of 20-100 $\text{mmol hr}^{-1} \text{mg}^{-1}$, mediated systems that use catalyst beds can generate hydrogen at substantially increased rates (up to 2861 $\text{mmol hr}^{-1} \text{mg}^{-1}$). The normalized H_2 -production rate is a commonly used metric for Type 2 systems and is summarized in **Table 2** for studies where it was reported. The turnover Number (TON) is the molar ratio of product made (H_2 or O_2) to active catalyst in the system and was calculated based on available information in each report.

Earth-abundant catalysts have also been used in the catalyst beds of Type 2 systems. Reactions can occur in the entire volume of a catalyst bed, rather than in a volume constrained to the near-surface region of an electrode, so higher loadings of catalysts can be beneficially utilized in catalyst beds than in electrochemical cells. Increased catalyst loadings decrease efficiency losses associated with catalytic overpotentials. Macdonald et al. investigated the use of Ni_5P_4 , Mo_2C , MoS_2 , and Ni_2P as HER catalysts in STA-mediated systems.²⁵ These catalysts yielded comparable results to Pt-based catalysts in STA systems. Similarly, Wu et al. investigated the use of CoP and Ni_2P as HER catalysts in STA-mediated systems, and observed comparable performance to systems that used Pt/C HER catalysts, both in terms of total hydrogen yield and rate of reaction (**Figure 6**).²⁶ CoP showed stability over 12 h of testing (**Figure 6b**).



Recently, STA-mediated systems were modified by Chisholm, Cronin, and Symes for use in a proton-exchange membrane (PEM) flow-cell configuration.²⁷ Through system optimization, the mediated electrolyzer operated at current densities in the range of 25–500 mA/cm². The level of H₂ in the O₂ stream was < 0.4% even when operated at a low current density (25 mA/cm²); by comparison the O₂ stream from a conventional PEM electrolyzer would contain > 2% if such a system were operated at the same low current density. (Typical PEM electrolyzers operate at current densities of 0.6 to 2 A/cm² and produce high-purity hydrogen.²⁸ For comparison, the safety threshold is 4 vol.% H₂ in O₂.) By monitoring the concentration of fluoride, a byproduct of Nafion breakdown, in the electrolyte over a 200 h period, the authors concluded that the decoupled system had an order-of-magnitude less membrane degradation than its coupled counterpart **Figure 7**. The spatial decoupling of the HER from the OER has been hypothesized to produce a lower concentration of reactive oxygen species, which are known to degrade ion-exchange membranes.²⁹

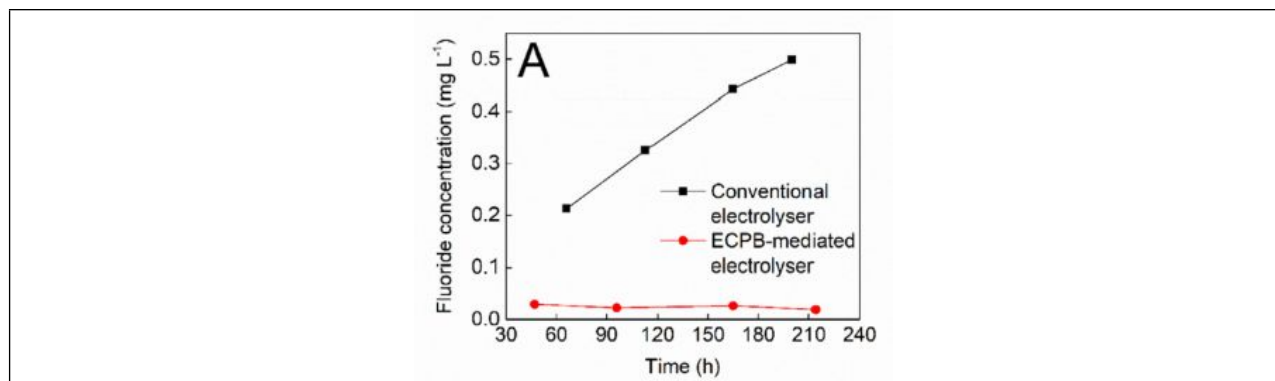


Figure 7. Comparison of fluoride concentration in solution measured as a function of time for a conventional electrolyzer and an STA-mediated electrolyzer. Fluoride is a product of Nafion breakdown. [Reprinted from Chisholm et al.²⁷ Published 2020 Elsevier. Licensed under a Creative Commons Attribution 4.0 license.]

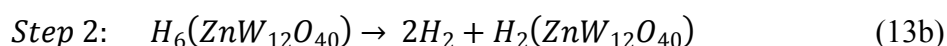
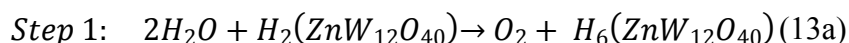
Even though the relevant redox peak of STA is located outside of the HER-OER potential window, the oxidation of STA and the coupled HER were performed electrochemically to enable efficient use in a PEM configuration; however, the approach could be used to generate hydrogen spontaneously in the second step.²⁴

Wu et al. utilized STA in decoupled aqueous systems that contained varied amounts of ethanol, DMF, or acetonitrile.³⁰ The inclusion of these solvents shifted the redox peaks of STA further negative of RHE, increasing the amount of hydrogen released upon exposure of STA to a Pt/C catalyst. The addition of ethanol in a 1:1 ratio with water increased the hydrogen produced in a single cycle from 45% to 85% of the maximum that could be produced if all the fully reduced STA were oxidized. Moreover, the hydrogenated STA could be used as a source of hydrogen for organic semihydrogenation, as opposed to typical semihydrogenation reactions that occur under an atmosphere of H₂(g). The selectivity for catalytic phenylacetylene hydrogenation to styrene was 80% at a conversion yield of 97%. Acetophenone was also catalytically hydrogenated to 1-phenylethanol at 82% selectivity at 80% conversion.

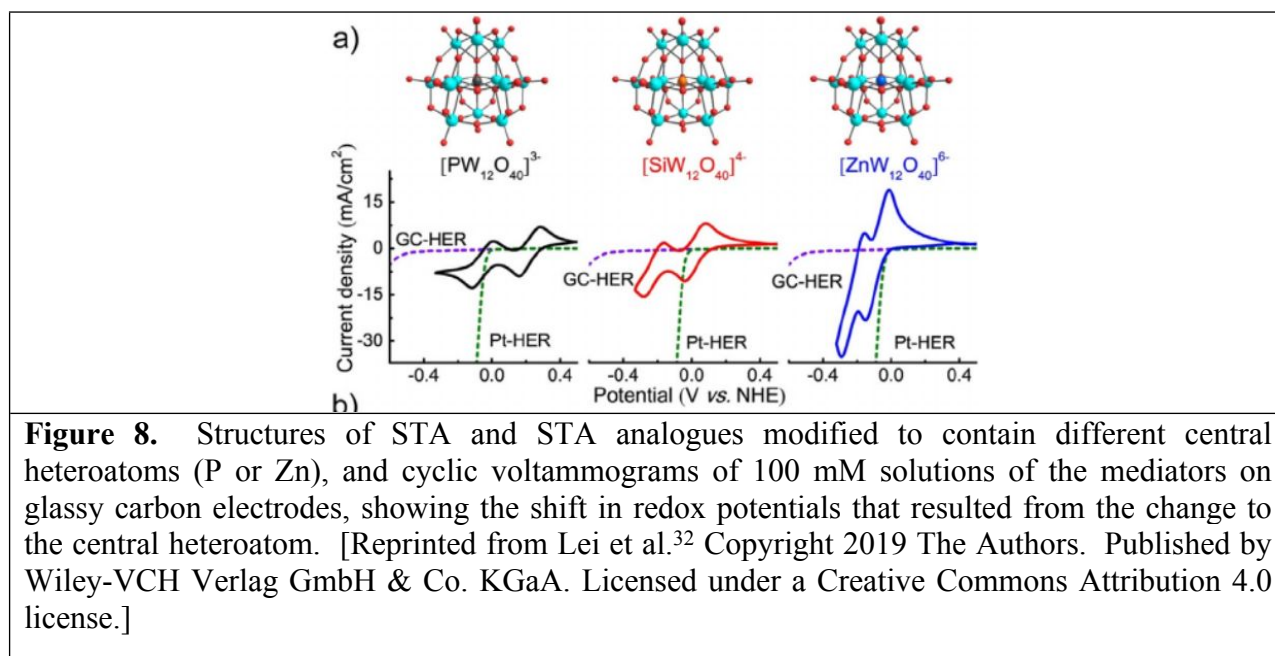
STA has also been utilized by Ma et al. in conjunction with Fe^{3+/2+} to operate a sunlight-driven RFB that splits hydrogen sulfide (H₂S).³¹ In this system, STA was reduced and Fe²⁺ was oxidized in a solar-powered RFB. CoP, FeP, and Ni₂P were mixed with the reduced STA to catalyze the spontaneous liberation of hydrogen. Simultaneously, introducing the Fe²⁺ to H₂S caused the generation of sulfur and protons, with the protons eventually transported to the HER

chamber to produce H_2 . The system maintained relatively stable operation for 100 cycles and achieved a maximum solar-to-hydrogen (STH) efficiency of 2.9%.

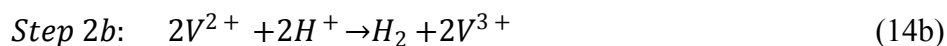
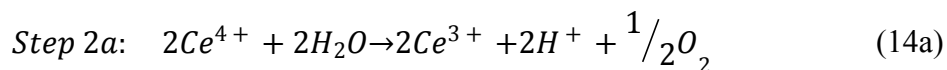
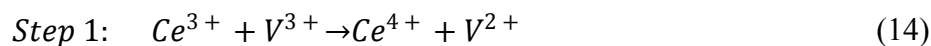
ECPB mediators other than STA have been reported for spontaneous hydrogen production. Macdonald et al. evaluated phosphotungstic acid (PTA), phosphomolybdic acid (PMA), and silicomolybdic acid (SMA) as mediators for the HER.²⁵ All three species have redox potentials more positive than that of STA, and thus were less effective, or completely ineffective, at spontaneously generating hydrogen. Lei et al. also reported the use of a different POM, $H_6ZnW_{12}O_{40}$ (ZTA), as a mediator.³²



Lei's investigation focused on shifts in the redox potentials of the mediator produced by changes in the central heteroatom (from P or Si to Zn) (**Figure 8**). In the case of ZTA, the negative shift of the redox potential placed both redox peaks negative of RHE. The long-term stability of the ZTA mediator was evaluated in a dual flow-cell configuration, and little degradation was noted after 200 cycles at constant current density.



Girault's group has focused on the use of redox couples commonly used in RFBs, such as vanadium and cerium.³³⁻³⁵ Amstutz et al. utilized a cerium/vanadium dual-circuit RFB for energy storage and water electrolysis.³³



In the charging step (Eq. 14), Ce^{3+} is oxidized to Ce^{4+} , while V^{3+} is reduced to V^{2+} , as in a conventional RFB. The charged electrolytes are stored until discharge is required, either by a conventional RFB discharge method or by passing the charged electrolytes through catalyst beds. When Ce^{4+} was passed through a bed of iridium or ruthenium oxide, oxygen spontaneously formed and Ce^{4+} was reduced back to Ce^{3+} (Eq. 14a). Likewise, when V^{2+} was passed through a Mo_2C bed, the oxidation of V^{2+} to V^{3+} was accompanied by the spontaneous generation of hydrogen. The discharged electrolytes can then be fed back into the RFB for recharging. Such a system provides increased flexibility and capacity for storage relative to a conventional RFB, because the Ce/V RFB can be “overcharged” during times of low electricity demand by converting excess charge to H_2 .

Recent reports have produced deeper insight into the functioning of spontaneous vanadium- and cerium-mediated systems. Reynard et al. studied the kinetics of spontaneous hydrogen production via oxidation of V^{2+} over a Mo_2C catalyst.³⁶ The reaction was studied for systematically varied ranges of vanadium concentration, vanadium state of charge, and catalyst loading, with kinetic rate laws developed for the process based on these parameters. The rate of spontaneous hydrogen evolution was found to be first-order in both the concentration of vanadium and the concentration of catalyst active sites.

The Modestino group has also evaluated $\text{Ce}^{3+/4+}$ as a redox mediator in decoupled electrolysis devices.³⁷ In their work, an electrolytic cell effected cerium oxidation concomitant with hydrogen evolution. A subsequent galvanic cell was used for spontaneous oxygen evolution and cerium reduction over the electrodes, allowing the excess power to be captured as usable electricity. At optimized species concentration, electrolyte flow rates, and operating temperatures, high faradaic efficiency (>90%) and low cell voltages (<1.8 V) were observed for a range of current densities from 0-150 mA/cm².

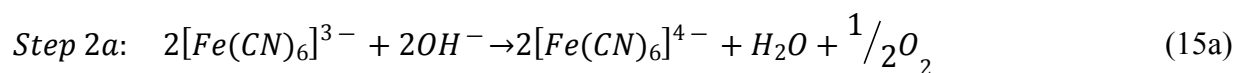
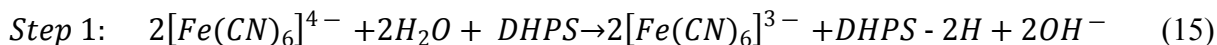
Following their initial report, Girault and Battistel shifted to working on RFBs that use vanadium as both redox couples.³⁴⁻³⁵ In such systems, the $\text{Ce}^{4+/3+}$ couple is replaced by $\text{V}^{5+/4+}$. The use of a vanadium-only system is desirable because the cerium species are more corrosive than the vanadium species, and issues associated with crossover of V or Ce are mitigated. The reversible redox potential of $\text{V}^{5+/4+}$ is more negative than that of $\text{Ce}^{4+/3+}$. Consequently, the all-vanadium RFB did not have sufficient voltage to spontaneously drive the OER half-reaction. The focus of the work thus shifted to developing other methods of discharging the positive vanadium electrolyte.

Peljo et al. studied replacing the OER in an all-vanadium dual-circuit RFB system with hydrazine, SO_2 , or H_2S oxidation.³⁴ Hydrazine provided a facile method to discharge the positive electrolyte, but with no economic benefit. SO_2 , a common industrial waste product, can be oxidized to form sulfuric acid in a catalyst bed or in a fuel-cell configuration. The catalyst bed is a simpler system for SO_2 oxidation than a fuel cell, but separation of the formed sulfuric acid from the RFB electrolyte adds complications. Oxidation of SO_2 in a fuel cell has its own drawbacks, including material crossover and catalyst degradation, but may be the more promising of the two options. H_2S was readily oxidized by the V^{5+} solution to form solid elemental sulfur, increasing the turbidity of the solution. Although the elemental sulfur is less desirable as a product than sulfuric acid, when paired with SO_2 oxidation, this approach could potentially provide a process for desulfurization of waste gas. The discharge of the positive V^{5+} electrolyte later was explored by creating a V- O_2 flow cell.³⁵ Discharge of the positive electrolyte of the V- O_2 flow cell required a minimum voltage input of 0.63 V at 10 mA/cm², unlike the spontaneous discharge of Ce^{4+} shown previously, but allowed for a system that only utilized vanadium-based redox species.³³

Xiang's group added solar energy inputs, a bipolar membrane, and pressurized hydrogen generation to the dual-circuit RFB concept.³⁸ In this system, the reduction of V^{3+} to V^{2+} over a carbon-cloth cathode in 2.0 M sulfuric acid was paired with water oxidation over a nickel anode in 2.5 M KOH. The bipolar membrane in the cell allowed use of anolytes and catholytes with mutually different pH values, and thus the pH of the electrolytes can be selected to optimize the stability and activity of the catalysts.³⁹ The discharge of the reduced vanadium species was performed using a Mo_2C catalyst, and hydrogen was collected at various pressures to simulate discharge at a central storage facility, a potentially beneficial alternative to the distributed

collection of hydrogen from an array of photoelectrochemical (PEC)⁴⁰ devices. The authors found that at 1, 10, and 100 atm, the amounts of hydrogen recovered from the vanadium solution were 83%, 65.2%, and 59.8%, respectively. All of the electricity required to run the cell was generated by a commercial solar cell illuminated by direct sunlight and guided by a solar tracker. The system operated at an overall STH efficiency of 3.7%.

Mediators other than vanadium and cerium also have been utilized in dual-circuit spontaneous oxygen- and hydrogen-evolution systems. Zhang et al. reported the use of 7,8-dihydroxy-2-phenazinesulfonic acid (DHPS) to mediate the HER on a Pt/Ni(OH)₂ catalyst and [Fe(CN)₆]³⁻ to mediate the OER on a NiFe(OH)₂ catalyst.⁴¹ In their system, reduction of DHPS and oxidation of [Fe(CN)₆]⁴⁻ occur simultaneously in a central flow cell, followed by spontaneous oxygen and hydrogen liberation in secondary reactor tanks.

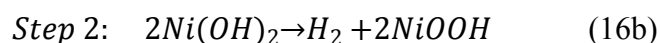
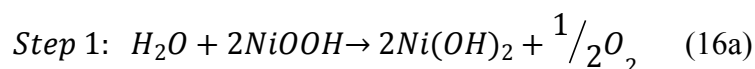


This dual-circuit system was operated in a strongly alkaline environment, in contrast to the acidic environments used for the vanadium- and cerium-mediated systems. Near-unity faradaic efficiency was maintained during continuous operation.

Type 3: Solid Mediator, Non-spontaneous

Table 3 lists the properties of mediators commonly used in decoupled water-splitting systems that use solid mediators (Type 3 and Type 4 systems).

Early reports of Type 3 systems came from Xia's group in 2016 and from Landman et al. in 2017.^{10, 42} Both groups used a nickel hydroxide auxiliary electrode to spatially and temporally decouple the HER from the OER in alkaline electrolytes. In both systems, the OER was paired with the reduction of the solid electrode from NiOOH to Ni(OH)₂, whereas the HER was paired with the reverse reaction:



Xia's system utilized a single Ni(OH)₂ electrode that was alternately wired to a Pt-coated electrode for the HER or to an IrO_x/RuO_x-coated electrode for the OER, all in the same cell. Landman's system incorporated two cells, each with a Pt-coated electrode and a NiOOH/Ni(OH)₂ electrode, in which the two Pt electrodes were connected to a power source and the Ni electrodes were wired together. In Landman's system, changing the polarity of the applied voltage switched the platinum electrode that was generating hydrogen into one that generated oxygen, and vice versa. A photovoltaic panel was used to drive decoupled water splitting at 7.5% STH efficiency. Although the standard potential for NiOOH/Ni(OH)₂ is ~ 100 mV positive of the thermodynamic potential of the OER, sluggish kinetics typical for the OER place the NiOOH/Ni(OH)₂ potential well below the onset of the OER, even with the best catalysts in alkaline conditions (~ 250-400 mV for ruthenium-based, iridium-based, or oxyhydroxide catalysts at 10 mA/cm²).^{39, 43-44} These sluggish kinetics required that both steps be run in non-spontaneous configurations. Similar to the idea later proposed by Ho et al.,³⁸ Landman envisioned decoupled electrolysis systems as being a beneficial method to centralize the hydrogen generation of an otherwise distributed PEC collection scheme (**Figure 9**).

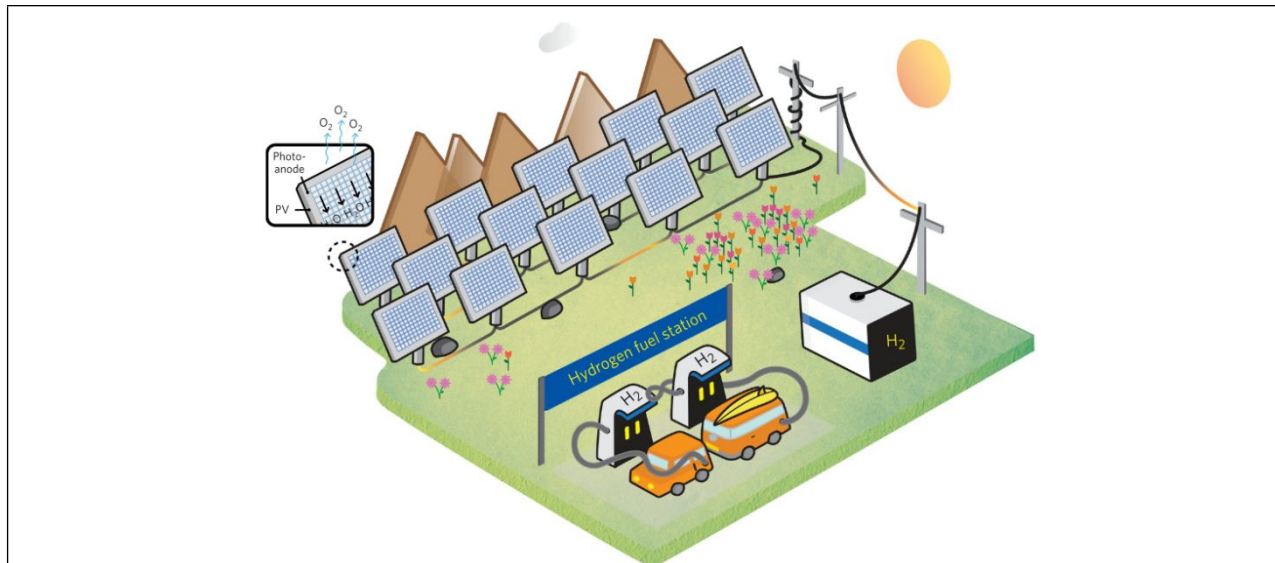
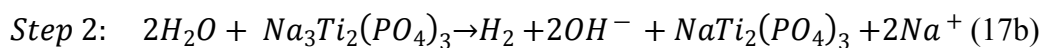
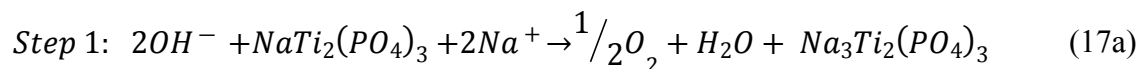


Figure 9. Proposed operation of a decoupled PEC water splitting array with a centralized hydrogen generator and fueling station [Reprinted with permission from Landman et al.⁴² Copyright 2017 Natural Publishing Group]

Further modifications to the NiOOH/Ni(OH)₂ system followed when Landman et al. utilized a PEC-PV stack to photoelectrochemically drive the decoupled reactions.⁴⁵ In this system, a PV-assisted hematite photoanode was used to drive the OER and reduce NiOOH. The reduced Ni(OH)₂ electrode was then moved to another cell where electrolytic hydrogen generation occurred. The initial PV module had a smaller surface area than the photoanode. When the PV module was scaled up to the same size as the hematite photoanode, the resulting increased current caused electrode instability. To alleviate this problem, a load was wired in parallel to the water-splitting modules, controlling the current passed by the electrolysis modules as well as allowing for generation of power.

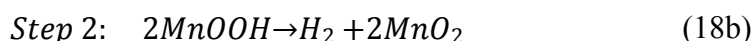
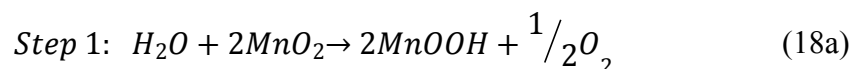
Guo et al. reported a membrane-free, two-electrode, decoupled electrolysis system mediated by either Ni(OH)₂ – as in earlier reports – or NaTi₂(PO₄)₃ (NTP).⁴⁶ The reversible Na⁺ intercalation of NTP gives:



In this system, an auxiliary mediator electrode was paired with a single a Ni₃S₂/CNT foam electrode that was utilized for both electrolysis half-reactions, as well as to reduce residual

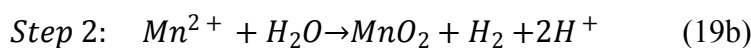
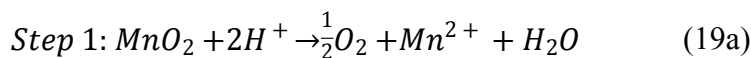
oxygen, with stable operation for 16-24 cycles, depending on the mediator. The Ni(OH)₂ mediated system was paired with a commercial Si PV module to achieve a maximum STH efficiency of 10.4% and stable operation for 7.5 h under simulated sunlight.

Other metal oxide electrodes in addition to NiOOH have been used for the solid-phase mediation of decoupled water splitting. Choi and Tsutsumi utilized a MnO₂ intermediate electrode for this application.⁴⁷



Here, the manganese oxide electrode was placed between a metal hydride cathode and a Ni(OH)₂ anode, separated by a polypropylene separator. The two outer electrodes were alternately connected to the auxiliary electrode to effect the water-splitting half-reactions.

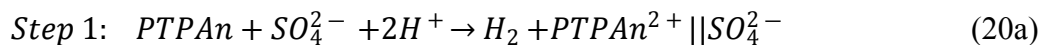
Huang et al. utilized a carbon felt auxiliary electrode to enable the plating and stripping of the MnO₂/Mn²⁺ couple to decouple electrolysis across a bipolar membrane.⁴⁸



A bipolar membrane was used so that the HER could occur in an acidic environment and the OER could occur in a basic environment, exploiting mutually favorable pH conditions in terms of activity and stability of the catalysts for the half-reactions. However, the voltage improvements gained by the improved activity of the catalysts were lost through other mechanisms, resulting in a decoupled system with 98.1% voltage efficiency compared to their acidic electrolysis analog.

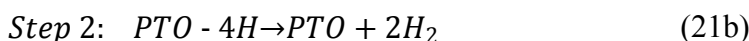
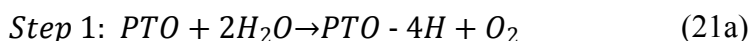
Jin et al. developed a decoupled water-splitting system that used FeO_x to alternately pair with acidic HER and alkaline OER.⁴⁹ The oxidation of metallic iron to Fe²⁺ and eventually Fe³⁺ was paired with the HER on a Pt/C electrode, then the reduction of Fe³⁺ back to Fe⁰ was paired with the OER on a Ni-Fe electrode. Overall, the FeO_x-mediated system had ~88.4% voltage efficiency. A TiO₂/Co-Pi photoanode was used to decouple water splitting at 3.3% STH efficiency at a current of 500 mA/g.

Organic mediators have also been used for Type 3 systems. Ma et al. reported the use of a polytriphenylamine (PTPAN)-based electrode for the solid-state mediation of decoupled water splitting in 0.5 M sulfuric acid:⁵⁰

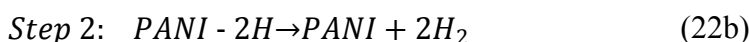
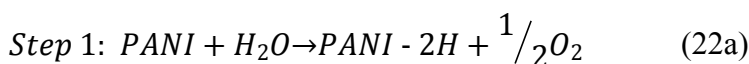


The decoupling strategy is the same as for other Type 3 systems, but the PTPAn electrode decouples the system by undergoing a reversible doping and de-doping process when the polarity of the applied bias is switched. In the first step (Eq. 20a), the HER is paired with the adsorption of sulfate anions from solution onto the PTPAn surface. In the second step (Eq. 20b), the OER is paired with desorption of sulfate into solution. This system was powered by a commercial Si solar panel, and exhibited 5.4% STH efficiency.

Other similar organic solid-state mediators have been investigated, including a pyrene-4,5,9,10-tetraone (PTO) auxiliary electrode⁵¹



and a polyaniline (PANI) electrode.⁵²



In both systems, the charge or discharge of a central electrode with redox peaks between the HER and the OER (Figure 10) is paired with the appropriate water-splitting half reaction. The PTO electrode functions by the reversible enolization of PTO,⁵¹ and the PANI electrode functions by reversibly transitioning through different doping states.⁵² In both cases, the systems were operated with power from commercial solar panels.

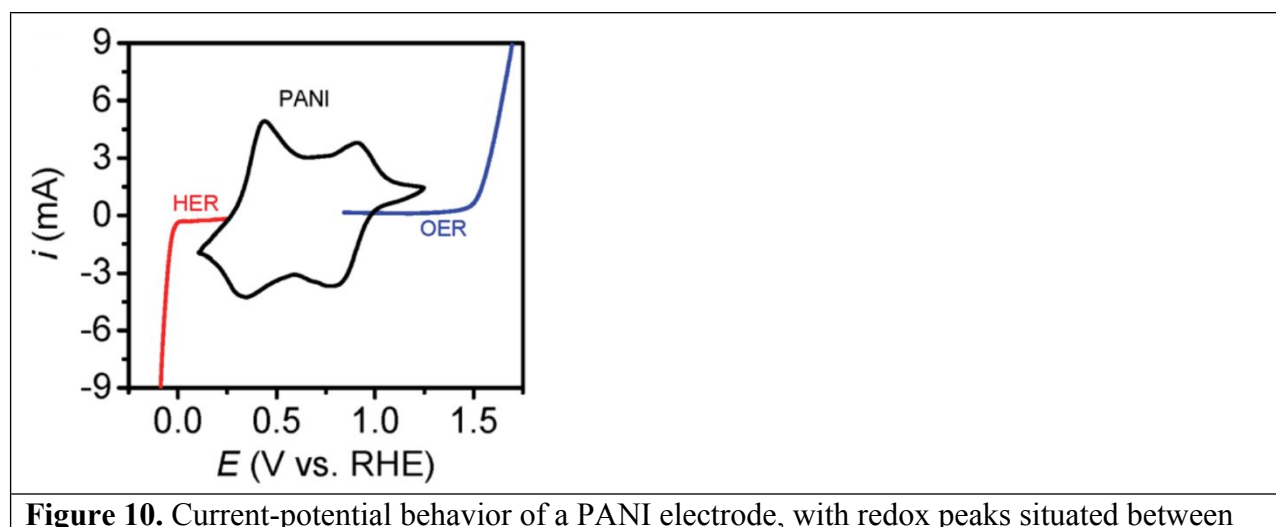
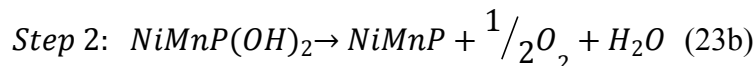


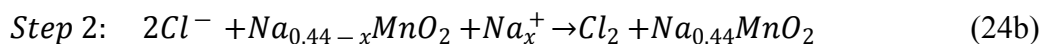
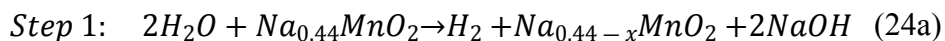
Figure 10. Current-potential behavior of a PANI electrode, with redox peaks situated between

the onset potential of HER and OER [Reproduced from Wang et al.⁵² with permission from The Royal Society of Chemistry]

Following earlier work focused on using layered double hydroxide (LDH) electrochemical capacitors (EC) for energy storage and electrolysis,⁵³ Liu et al. utilized an electrochemical pseudocapacitor in decoupled sunlight-driven water-splitting applications by using a Ni-Mn-P electrode.⁵⁴ Pseudocapacitors utilize reversible electrochemical reactions on or near high-surface-area electrodes for energy storage, as opposed to ECs that utilize electrochemical double-layer capacitance for energy storage.⁵⁵ In the reported system, 1.6 V was applied across the Ni-Mn-P and Ni₂P electrodes to charge the Ni-Mn-P with OH⁻ and drive the HER on the Ni₂P. After charging for 10 min, the Ni-Mn-P electrode was discharged, releasing OH⁻, and driving the OER over the Ni₂P electrode with minimal voltage input of ~0.17 V. As with the NiOOH mediated systems, sluggish OER kinetics require both steps to be run non-spontaneously, even though the potential is slightly more oxidative than the thermodynamic potential for the OER (+0.07 V)



Xia's group expanded solid-mediated systems by replacing the OER with the chlorine-evolution reaction (CER).⁵⁶ In this system, a sodium-doped MnO₂ electrode was used as a solid-state mediator to decouple the HER from the CER. First, the electrolytic HER was paired with de-intercalation of sodium from the auxiliary electrode in 1 M NaOH. The MnO₂ electrode was then moved to a saturated NaCl solution, where intercalation of Na was paired with chlorine evolution.



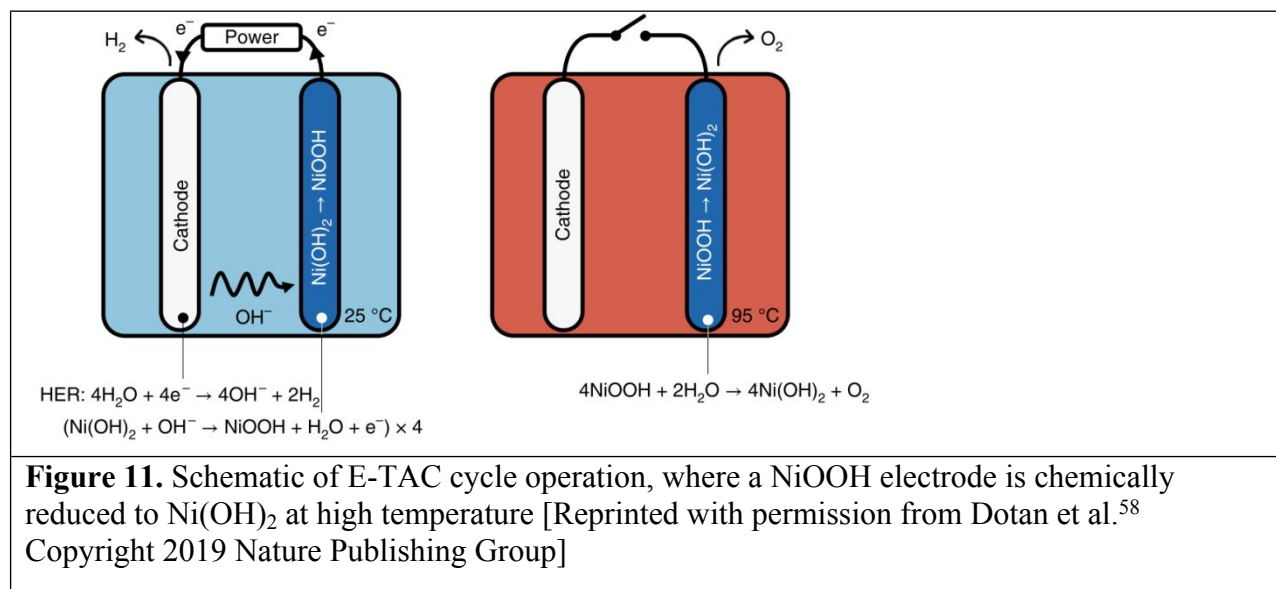
The approach thus resulted in a membrane-free chloralkali process.

Other solid-state reversible redox reservoirs have been demonstrated for use in modular electrochemical synthesis schemes.⁵⁷ Wang et al. utilized sodium nickel hexacyanoferrate (Na-NiHCF) as a mediator for the production of hydrogen peroxide that did not produce O₂ or H₂, which are the usual byproducts of electrochemical hydrogen peroxide and sodium persulfate

synthesis, respectively.⁵⁷ This modular electrochemical synthesis operated stably for over 100 cycles.

Type 4: Solid Mediator, Spontaneous

Grader and Rothschild expanded upon their earlier Ni(OH)₂ work⁴² by changing the process through which NiOOH is reduced back to Ni(OH)₂.⁵⁸ The first step involved the electrolytic oxidation of electrodeposited Ni(OH)₂ to NiOOH paired with the HER.⁴² The reduction of NiOOH back to Ni(OH)₂ occurred in a subsequent chemical step by submersion in water at 95 °C, which simultaneously liberated oxygen gas. In this work, the Ni(OH)₂ anodes were doped with small amounts of cobalt, giving anode compositions closer to Ni_{0.9}Co_{0.1}(OH)₂. Cobalt doping of nickel hydroxide electrodes was found to negatively shift the oxidation peak of Ni(OH)₂ by about 50 mV, reducing the parasitic OER during electrode charging. The thermodynamic potential for reduction of cobalt-doped NiOOH is more positive than the thermodynamic potential for the OER, but the reaction is kinetically unfavorable at room temperature. Increasing the temperature of the electrode activates the chemical step of oxygen evolution, completing an electrochemical – thermally-activated chemical (E-TAC) cycle. When the nickel auxiliary electrode is shuttled between a hot cell and a cell at room temperature, the net reaction is the same and produces overall water splitting. With proper insulation, such a system could operate with minimal energetic input to maintain the temperature of the heated bath. This technology is being developed for commercialization by H2Pro, which utilizes an E-TAC process to generate pressurized hydrogen in a membrane-free system.⁵⁹



Recent work from Landman et al. focused on improving their previous E-TAC system by replacing the electrodeposited Ni(OH)₂ anodes with core-shell electrospun nanofiber Ni(OH)₂

anodes.⁶⁰ These high-surface-area nanofiber anodes were also doped with cobalt to shift the Ni(OH)_2 oxidation peak to more reductive potentials, allowing for deeper electrode charging without parasitic oxygen evolution. Compared to their previously reported electrodeposited anodes, both the undoped and cobalt-doped nanofiber anodes substantially outperformed the electrodeposited material in terms of regenerated charge and current density when normalized by volume, anode area, or total mass. The nanofiber anodes slightly outperformed the electrodeposited anodes when normalized by active layer mass at long charge and discharge timescales of 800 seconds.

Xia's group expanded upon their previous Ni(OH)_2 work¹⁰ by replacing the OER with the oxidation of ethanol.⁶¹ In this system, the electrolytic HER is again paired with oxidation of Ni(OH)_2 . The oxidized nickel electrode is then moved to a new cell in which the reduction of NiOOH to Ni(OH)_2 is paired with the ethanol-oxidation reaction (EOR). Due to the onset of the EOR potential at 0.26 V vs. RHE, the second step occurs spontaneously. The EOR provides substantially more electrochemical potential than is required to reduce NiOOH , so additional power can be siphoned off as electricity.

Tangentially Related Technologies

Numerous technologies have been reported that are outside of the scope of this review but are related tangentially to decoupled water splitting. These include, but are not limited to, heterogeneous photocatalytic water splitting,⁶² Z-scheme water splitting,⁶³ hybrid bioinorganic solar fuels schemes,⁶⁴ decoupled bioelectrochemical systems,⁶⁵⁻⁶⁶ decoupled thermochemical water splitting with an iodine and sulfur cycle,⁶⁷ redox-mediator-assisted electron transfer,⁶⁸ mediator-assisted photochemical H₂S splitting,⁶⁹ POM-based CO₂ reduction catalysts,⁷⁰ and more. Others have developed conventional batteries that use one or both water-splitting half-reactions to increase system flexibility. Of these tangentially related technologies, these flexible battery systems are most similar to decoupled water-splitting systems and are thus discussed further.

In an initial report on NiOOH as a solid-state redox mediator, Xia's group also demonstrated that NiOOH could be coupled with a zinc anode to create a NiOOH-Zn battery.¹⁰ After discharging, the reduced Ni(OH)₂ was paired with an HER catalyst to electrolytically generate hydrogen and oxidize the nickel back to NiOOH, restarting the cycle. Operating in this way, recharging the nickel side of a NiOOH-Zn battery simultaneously generated hydrogen. Similarly, Xia's group further reported a decoupled amphoteric water-electrolysis system that included integration with an Mn-Zn battery.⁴⁸ This integration allowed for flexible electrical storage and energy conversion by pairing battery charging half-reactions with electrolysis half-reactions.

Similarly, in Huang et al.'s report of a Cu-Mn battery, a second operational mode was introduced to the otherwise standard battery.⁷¹ Under standard operation, battery charging occurs with the oxidation of Mn²⁺ to MnO₂ paired with the reduction of Cu²⁺ to Cu. The discharge step involves the opposite process. In the decoupled electrolysis configuration, during charging the Cu plate was replaced with a HER catalyst, such as Pt. The charging of the Mn side of the battery was thus paired with hydrogen generation, whereas the discharging of the battery behaves conventionally.

Mulder et al. designed a "battolyser" system, which was the integration of a Ni-Fe battery and an electrolyzer.⁷² In standard operation, this system had Ni(OH)₂ and Fe(OH)₂ electrodes in an alkaline environment. The charging process paired the reduction of Fe(OH)₂ to Fe and the oxidation of Ni(OH)₂ to NiOOH. The battolyser can be charged to capacity, then discharged as a

standard battery. At times of increased energy generation or reduced energy demand, when a standard battery would sit idle and full, the battolyser was operated as an electrolyzer. In this secondary function, the now-reduced Fe electrode acted as a HER catalyst and generated $\text{H}_2(\text{g})$, while the NiOOH electrode acted as an OER catalyst and generated $\text{O}_2(\text{g})$. In this manner, “overcharging” of the battery resulted in making hydrogen, ensuring that any excess energy input (potentially from sunlight) is not wasted when the battery is full. In a follow up to the battolyser, Weninger and Mulder added additional hydrogen-evolving and oxygen-evolving electrodes (HEE and OEE).⁷³ In this approach, the same $\text{Ni}(\text{OH})_2$ and $\text{Fe}(\text{OH})_2$ electrodes are used as battery electrodes, but the new electrodes are wired in parallel with them – the HEE on the Fe side and the OEE on the Ni side. By changing the state of charge of the battery and reconfiguring the connections to the four electrodes, the battolyser-type system can perform as a battery, an electrolyzer, or a half battery/half electrolyzer. In this approach, many combinations of OER, HER, half-charging, and half-discharging can be paired with one another, creating a single device with high flexibility to respond to generation and demand.

Discussion and Prospective

Decoupled water-splitting systems contain more process components than conventional electrolyzers, including RFBs, catalyst beds, and auxiliary electrodes, as well as mass flow equipment such as piping, pumps, and solid-conveying systems. The systems sometimes utilize expensive and low-durability mediator materials. It is not known whether the stated potential benefits of decoupled water-splitting systems – such as flexibility and modularity – can outweigh costs associated with increased system complexity. For these systems, the cost-benefit analysis is a moving target, as innovation will continually – and perhaps unevenly – drive down costs of both conventional electrolysis and decoupled water-splitting systems.

Potential Benefits for Conventional Grid Electrolysis:

Separators:

Grid-powered electrolyzers are mature and well-known technologies that are operated continuously and at high current densities. In alkaline electrolysis, an ion-permeable separator is used to permit flow of ions between the anode and cathode without allowing for the crossover of H₂ or O₂ to the other chamber, which would create an explosive gas mixture. In PEM electrolysis, a Nafion membrane permits separation of the gases while allowing proton transport to occur with minimal ohmic resistance losses. In solid-mediated decoupled systems (Type 3 and 4), a separator is not required because H₂ and O₂ are not formed at the same time and place. This is also true for Type 3 and 4 systems that generate pressurized hydrogen.

In conventional electrolyzers and fuel cells, gas crossover can lead to the formation of reactive oxygen species (ROS), such as hydrogen peroxide, HO*, and HOO*, which are known to contribute to membrane thinning.^{29, 74} A report from Fouda-Onana's group found that membranes in PEM water electrolyzers can lose half of their initial thickness in approximately one year when operated at 333 K and 1 A/cm².⁷⁴ Other reports have identified the membrane-electrode assembly as the weakest part of a PEM system,⁷⁵ and have attributed the previous shut-down of a commercial electrolysis process to high hydrogen crossover due to substantial Nafion membrane thinning and eventual membrane failure.⁷⁶ The increased risk of mechanical failure and the diffusive crossover of gases through the thinned membrane can decrease fuel yield and cause unsafe levels of gas mixing to occur, necessitating the replacement of the membrane.

Operating a decoupled electrolysis system reduces the possibility of ROS being formed, and has been shown to substantially reduce the amount of fluoride found in the electrolyte, a sign of the degradation of the fluorinated Nafion membrane.²⁷

In liquid-mediated systems (Type 1 and 2) a separator is required to keep the mediator isolated in its proper half-cell. However, the separator in these systems may need to be impermeable only to the mediator, and not to H₂ and O₂. In cases where the mediator has a high molecular weight, such as PMA at 1825 g/mol, specialty high-performance membranes like Nafion can in principle be replaced with cheaper benzoylated cellulose dialysis membranes.¹¹ In systems that use more expensive membrane separators, such as those mediated by HQS¹⁵ or V,³³ a decoupled electrolysis scheme may potentially increase the lifetime of the separator by reducing the formation of ROS. The tradeoff of increasing system complexity to enable the removal or replacement of a separator depends on the cost and longevity of the conventional separator relative to the new system components.

Membrane-Free Generation of Pressurized Hydrogen:

Vehicular integration, long-distance transport, and some industrial applications commonly require hydrogen at 200, 350, and 700 bar of pressure.⁷⁷ An NREL analysis of the economic feasibility of a hydrogen compression, storage, and dispensing (CSD) network claimed that hydrogen compression comprised over 50% of the capital costs and over 25% of the energetic cost of the system, with specifics depending on the model and scenario.⁷⁸ Other estimates have placed the minimum energetic cost of hydrogen compression between 5-20% of the total energetic content of the hydrogen being compressed, depending on the compressor type and final pressure.⁷⁹ The same report estimated the energetic cost of hydrogen liquification to range from 30-40% of the LHV of hydrogen.

PEM electrolyzers can produce hydrogen at high pressure, either in balanced or differential pressure modes.^{2, 28} Differential pressure mode, in which the anode and cathode sides of the electrolyzer are operated at mutually different pressures, can be utilized to reduce system cost and complexity. However, high differential pressures can produce higher gas crossover and may increase the likelihood of membrane thinning or separation failure.^{74, 80} Although higher pressure lab-scale systems have been demonstrated, for these and other mechanical reasons the pressure in commercial PEM electrolyzers appears to be limited at present to ~30 bar.⁸¹⁻⁸²

Decoupled electrolysis can be used to generate hydrogen under pressure without the use of gas-impermeable membranes. The French start-up ERGOSUP utilizes a Type 3 system to generate pressurized hydrogen in an intrinsically safe, membrane free unit,⁸³ whereas the Israeli start-up H2Pro does the same with a Type 4 E-TAC system.⁵⁹ H2Pro has stated that their E-TAC technology can support hydrogen production at pressures in excess of 100 bar, which in certain applications could reduce the compression ratio required, or possibly eliminate the need for a compressor entirely. The full cost advantages of such a system will depend on the scale and type of application, because in some cases the cost of compression can be ~10% of the cost to make the hydrogen, and in turn the components of the electrolyzer that produce high pressure hydrogen would need to be made out of more costly materials to safely confine the high pressure gas produced by the decoupled electrolyzer system.

Catalysts:

For Type 2 systems, the HER can be performed chemically in a catalyst bed. Higher loadings of high-surface-area catalysts can be obtained on catalyst beds than on an electrode surface. Incorporation of precious metal catalysts on highly porous supports can substantially reduce the loading of catalyst needed to achieve facile generation of hydrogen. Conventional electrolyzers in laboratory environments have shown hydrogen-generation rates of 20-100 mmol h⁻¹ mg⁻¹, compared to values from 1000-3500 mmol h⁻¹ mg⁻¹ in decoupled systems using precious metal catalysts.^{13, 24} In Type 2 systems, earth-abundant catalysts have demonstrated hydrogen-production rates up to 10 mmol hour⁻¹ mg⁻¹, which could allow for the utilization of inexpensive earth-abundant catalysts in a grid-scale electrolyzer scheme that does not require precious metals.²⁵⁻²⁶

In Type 1 systems that used non-precious metal electrodes, the systems approached the voltage efficiency of precious metal electrodes in a conventional electrolysis scheme.¹⁵ Combining the approach with a scheme to reduce the mediator without coupling to the OER, such as the use of POM mediators in wood-pulp bleaching,⁸⁴ could provide an opportunity to develop a Type 1 system that does not involve precious metal electrodes. The replacement of precious metal catalysts with earth-abundant catalysts, or the drastic reduction of the required

amount of precious metal catalysts, may be beneficial to grid-powered electrolyzers if the reduction in cost can outweigh the inclusion of more process steps.

Furthermore, the use of catalyst beds relocates bubble formation from an electrode surface, which can occur in conventional alkaline electrolysis, to the catalyst bed. Bubbles cause efficiency losses by blocking active areas of the electrode surface and by increasing the effective resistance of the electrolyte in which the bubbles are formed.⁸⁵ Model work has shown that oxygen bubbles block catalyst sites in PEM water electrolysis systems, decreasing the active surface area and increasing the effective OER overpotential in the range of 28-43 mV, depending on the type of bubble.⁸⁶ Elimination of these types of losses could be an added benefit provided by the use of catalyst beds.

Alternate Reactions:

In many conventional and decoupled electrolysis systems, oxygen is considered a low-value byproduct of hydrogen evolution and is thus released to the atmosphere. Given the modularity of decoupled electrolysis systems, the value-added HER can be paired with virtually any electrochemical oxidation reaction instead of the OER, including chlorine evolution,⁵⁶ wastewater treatment,²¹ H₂S splitting,³¹ SO₂ oxidation,³⁴ HMF oxidation,²³ or ethanol oxidation.⁶¹ This concept of modular electrochemical synthesis has been expanded beyond water splitting reactions, such as mediator-paired hydrogen peroxide and sodium persulfate synthesis.⁵⁷ Details of these systems have been covered throughout this review as well as in other reports.³ The modularity of these systems could allow for rapid switching between various electrochemical reactions when feedstocks or power provision make it economical to do so.

The generation of a higher-value oxidation product may introduce trade-offs that are not considerations for oxygen-evolving systems. Increased system complexity and the inclusion of more corrosive feedstocks or products will increase the system cost. Depending on the reaction, it is likely that the chemical feedstock will be more expensive than water, potentially offsetting any economic advantage of generating a higher-value oxidation product with such approaches. As with other proposed benefits of decoupled electrolysis systems, the feasibility of utilizing redox mediators to enable oxidation to value-added chemicals in a flexible and modular operating scheme requires a full cost-benefit analysis.

Other Cost Improvements:

Current cost estimates for industrial hydrogen produced from PEM and alkaline electrolysis are \$4-6/kg H₂. The range depends on differences in electricity cost, capacity factor, and scale of electrolyzer production, with the most optimistic future projections placing the cost between \$2-3/kg H₂.⁸⁷⁻⁸⁹ Manufacturing-cost breakdowns for the two types of systems are similar, with balance-of-plant and stack costs contributing roughly equally to overall system cost. The cost of hydrogen production in these systems varies linearly with the price of electricity until capital costs dominate the levelized cost of hydrogen.

Limited work has been conducted in analyzing the ways that decoupled electrolysis systems could become cost-competitive with conventional PEM electrolyzers. In the Frey et al. techno-economic analysis of a cerium-mediated dual-cell electrolytic-galvanic decoupled electrolysis system, experimental data from custom flow cells were used to find cost-optimal operation schemes using real US electricity prices, resulting in decoupled electrolysis H₂ prices in the range of \$4-5/kg H₂.³⁷ Generally, system costs were reduced when operating the electrolytic (charging) HER cell during times of low-price grid electricity, and operating the galvanic (discharging) OER cell during times of high electricity price. In some scenarios, the overall electricity costs were lower than state-of-the-art PEM electrolyzers, which they estimated to produce hydrogen at approximately \$2.30/kg H₂.³⁷ However, the reduction of electricity cost compared to PEM electrolyzers was still vastly outweighed by the increased capital cost required to utilize two electrochemical cells (HER + Ce oxidation / OER + Ce reduction) instead of one (HER + OER). Future developments and engineering improvements associated with scale-up of what are currently proof-of-concept devices will be beneficial to substantially closing cost gaps between PEM electrolyzers and decoupled systems.³⁷

Storage-Density Improvements:

Once a conventional electrolyzer makes hydrogen, the gas must be stored for later use. This step can be facilitated by pressurizing the hydrogen or condensing it into a cryogenic liquid, which has a density of 71 g H₂/L. Because many of the mediators uptake protons when they are reduced, they can be thought of as hydrogen-storage systems. Of the mediators considered, lithium polyoxoanion, Ni(OH)₂, and MnOOH have hydrogen-storage densities of 34.2, 44.2, and

57.9 g H₂/L, respectively. These mediators can be pumped or transported to a location for hydrogen discharge without the potential for the accidental release of hydrogen or hydrogen leaks during transit.

Safety Improvements:

Catastrophic failures resulting from the flammability of hydrogen have occurred across many industries, including chemicals,⁹⁰ nuclear power,⁹¹ and aviation.⁹² The spatial and temporal co-generation of hydrogen and oxygen can lead to an unsafe mixture of the two gases, creating a potential explosion hazard. The degradation or failure of separators or membranes in electrolysis systems, especially those under pressure, is a well-known failure mechanism of electrolyzers.⁷⁵⁻⁷⁶ A decoupled electrolysis system essentially eliminates the possibility of generating an explosive hydrogen-oxygen gas mixture, and can also reduce costs of the materials required for safe operation of electrolyzers that contain potentially explosive hydrogen/oxygen mixtures and high pressures of hydrogen gas.

Potential Benefits for Solar-Powered Electrolysis Systems:

Direct solar-powered electrolysis systems that are not connected to the electrical grid and that do not use conventional electrolyzers differ fundamentally from grid-powered electrolysis systems, in that the former systems can only operate when the sun is shining. These technologies are far less mature than conventional electrolysis systems and therefore any discussion of techno-economic tradeoffs would be highly speculative. However, some of the technical advantages of decoupled water-splitting systems suggest that these modular systems may prove at least as feasible as photoelectrochemical (PEC) water-splitting systems.

Separators:

Photoelectrochemical electrolysis systems that are powered directly by unconcentrated sunlight will operate at current densities of tens of mA/cm², as limited by the photon flux of the insolation. In contrast, grid-powered electrolysis units operate in the A/cm² range. Operating under intermittent, low-current-density conditions creates efficiency and safety issues due to the intrinsic crossover of H₂ and O₂ through membranes and especially through highly gas-permeable separators. The crossover of gas through a low-permeability membrane is a function of the concentration of that gas in the contacting liquid.⁸⁰ Aqueous environments become saturated with hydrogen at low concentrations,⁹³ so the rate of crossover does not appreciably change as current density increases or decreases. At low current density, the amount of oxygen generated decreases, whereas the amount of hydrogen entering the anode chamber does not change. In the absence of a mitigation strategy, the concentration of hydrogen therefore continually increases in the anode chamber as current density decreases.^{74, 80} In the report of a decoupled PEM system by Chisholm et al., the fraction of hydrogen in the oxygen side of a conventional electrolyzer increased from 1.47% to 1.89% when the current density was lowered from 50 to 25 mA/cm². In contrast, at both current densities the amount of hydrogen on the oxygen side of the decoupled PEM system was only 0.31%.²⁷

Aside from safety concerns, the substantial crossover of hydrogen at low current densities causes a reduction in efficiency due to loss of fuel. Modeling work from Berger et al. demonstrated that the net quantity of hydrogen evolved by a PEC device would increase substantially, from <4 mA/cm² to >6 mA/cm², when the hydrogen-permeation coefficient of the membrane was reduced from that of Nafion to a hypothetical membrane that had a permeation

coefficient of 0.01.⁹⁴ A decoupled photoelectrochemical system would have no hydrogen crossover, leading to the same increase that could be achieved through use of an improved membrane.

Centralized Generation of Hydrogen:

Some proposed designs for photoelectrochemical systems rely on the distributed generation of hydrogen in cheap, integrated, tandem-junction devices that would span large areas. Water would be split across the entire device, requiring hydrogen to be collected over a vast area. An integrated photoelectrochemical system could be used to reduce a liquid mediator¹⁷ while generating oxygen using a semiconducting crystal such as BiVO_4 ¹⁸⁻¹⁹, and the reduced mediator could be pumped to a central location, where hydrogen could be liberated under pressure. A liquid mediator is potentially less expensive to transport safely than hydrogen gas, which would require H_2 gas-tight collection systems and pressure-management technologies to collect. Decoupled water splitting could obviate the need for photoelectrochemical water-splitting systems to be gas-tight, as the produced oxygen can be released to the atmosphere. The spontaneous, pressurized generation of hydrogen from a mediator at a central location has been shown by Ho et al.,³⁸ and could be important to realizing a functioning and economically feasible photoelectrochemical water-splitting system because pressurization of hydrogen produced at atmospheric pressure is energy-intensive.⁹⁵⁻⁹⁶

Flexibility:

An oft-cited issue with systems powered by wind or solar electricity is intermittency. An electrolyzer only coupled to solar energy input would operate at a low power density and moreover would be subject to the variability of the renewable energy input. Decoupled electrolyzer systems could have increased operational flexibility relative to their coupled counterparts, which may be a useful asset in systems that are powered solely by sunlight. Deconstructing the water-splitting reactions into two non-spontaneous steps reduces the instantaneous power that is required to operate the system, which may be beneficial in interfacing the system with variable renewable energy sources. The physical and temporal isolation of the two half-reactions could allow for day-night cycling in which one water-splitting product is made during the times of peak solar insolation (6 h), while the other product is made

slowly (18 h). The ability for some systems to “overcharge” RFBs with minimal additional unit operations could potentially facilitate integration of these systems. The flexible battery systems allow for quick shifting between various modes of operation, which could be utilized to rapidly adapt to changes in energy input or demand. The analysis of any economic benefit of increasing operational flexibility at the expense of increased system complexity needs careful analysis and consideration. Cost breakdowns versus scale for both alkaline and PEM electrolyzers for use in grid-connected electrolysis are available and serve as a starting point for assessing any advantages or disadvantages of alternative designs or systems for water splitting.

Conclusions

Decoupled water splitting is a new and growing field focused on exploring how separating the electrochemical oxygen- and hydrogen-evolution reactions – either spatially, temporally, or both – can benefit electrolysis systems used for generating carbon-neutral hydrogen. From the field’s inception in 2013, a vast range of mediators, catalysts, separators, electrochemical environments, light absorbers, and engineering optimizations have been implemented, creating a diverse group of systems for consideration. Research in decoupled water splitting has benefited from methods that have been known for decades in related fields, such as (photo)electrochemistry and heterogeneous catalysis. Similar research challenges are found across these fields, such as high OER overpotential and the longevity of device components.

Numerous types of decoupled electrolysis systems have been explored. These systems have allowed for earth-abundant catalysts to generate hydrogen at rates approaching that of precious metal catalysts in PEM electrolysis systems. Membrane separators have been replaced with cheaper alternatives or removed entirely, depending on the system. Membrane-free production of pressurized hydrogen has been achieved. Some mediators have energy- or hydrogen-storage densities that are approaching that of cryogenic hydrogen, albeit with an electrochemical penalty for accessing that hydrogen. Oxygen evolution has been replaced with other value-added oxidation reactions, with mediators further implemented in completely modular electrochemical synthesis schemes. The intrinsic safety and operational flexibility of electrolysis have been substantially improved as well.

Elements of decoupled water-splitting systems may also be exploited beneficially in unassisted photoelectrochemical water-splitting systems. PECs operate at low current density

compared to conventional electrolyzers, and decoupled systems have shown the most improvement to membrane stability and gas crossover when the current density is low. Furthermore, the collection of gaseous hydrogen over a vast array of PEC devices is a difficult engineering feat, which may be alleviated by redox-mediated generation of hydrogen in a central facility. In either case, the modularity and flexibility of decoupled electrolysis systems can enable the rearrangement of electrochemical reactions and facilitate changes in the aqueous environment in PECs, which may decrease reaction overpotentials or increase semiconductor stability.

Technical hurdles and knowledge gaps for the implementation of decoupled electrolysis devices still exist. As is the case with photoelectrochemical electrolysis research, quantifying the long-term performance of a device is non-trivial. Generally device performance has been evaluated for dozens of cycles over the time scale of days at most, which is far from the decades-long timescale that is needed for grid-scale electrolyzers. Use of earth-abundant catalyst beds in Type 2 systems has been primarily investigated in proof-of-concept systems that have focused on demonstration and determination of the initial rate of hydrogen production, with rigorous kinetic studies only being introduced relatively recently. Values for turnover numbers gleaned from the available data have shown $\text{TON} < 10$ for several earth-abundant catalysts, leaving in question the long-term performance of such materials. However, these studies were not focused on improving the TON, so these values should be considered as a lower bound. Many decoupled electrolysis systems require the movement of charged liquid or solid mediators, both of which introduce logistical and thus cost concerns. The impact of corrosive mediators has been mentioned briefly, but the economic impact on the longevity of hardware or the requirement of using more expensive components has not been analyzed. These and other unanswered questions, of both a fundamental scientific and practical engineering nature, stand between full utilization of decoupled water splitting systems in clean, industrial hydrogen generation.

Substantial opportunity exists for developments in the field. Studies focused on quantifying the long-term performance of systems, either through more fundamental analysis of degradation pathways or careful analysis of failure, can give necessary insight into practical implementation of such systems. Type 4 systems are the least explored category yet may prove to be valuable technologies as both Type 2 and Type 4 systems spontaneously drive half of the overall water-splitting reaction. Driving spontaneous half-reactions gives these systems the

ability to pair directly with solar power in the day, followed by the spontaneous reaction at night. Development of a Type 2 system that utilizes a photocatalyst to drive the non-spontaneous step, followed by a catalyst bed to drive the spontaneous step, would result in a completely electrode-free electrolyzer, with the only power inputs being solar illumination and pumping liquids. Given the modularity of decoupled water splitting systems, these and other designs may combine favorable performance characteristics of related electrochemistry fields. A caveat is whether the cost savings from these potential benefits outweigh the cost of increasing system complexity.

Acknowledgments

This material is based upon work performed by the Joint Center for Artificial Photosynthesis, a DOE Energy Innovation Hub, supported through the Office of Science of the U.S. Department of Energy under Award Number DE-SC0004993. MCM acknowledges Graduate Research Fellowships from the National Science Foundation and the Resnick Sustainability Institute at Caltech.

Table 1. Properties of soluble mediators used in decoupled water-splitting systems.

Mediator	E° (V vs. RHE)	pH	Proton balance	Conc. Range [M]	H ₂ Density [g H ₂ /L]	Stability [cycles] (Retained Capacity)	Ref.
PMA	0.57, 0.68	0.3	Yes	0.01 – 0.5	0.02 – 1	4 (97%)	11-12, 17-18, 25
LiPWO	-0.38, -0.15, 0.1, 0.27	0	Yes	0.002 – 1.9	0.04 – 34.2	100 (97.3%)	13
HQS	0.69	0.7	Yes	0.5	1	20 (80%)	15
AQDS	0.21	0	Yes	0.025 – 0.5	1	100 (94.25%)	16
Fe ^{3+/2+}	0.92	2.6	No	0.005 – 4.3	0.005 – 4.3	-	19, 31
[Fe(CN) ₆] ^{3-/4-}	1.19 – 1.37	7 – 14	No	0.25 – 0.7	0.25 – 0.7	-	20-21, 23, 41
FcNCl	1.01	6.5	No	0.05 – 4	0.05 – 4	20 (100%)	23
STA	-0.20, 0.04	0.6	Yes	0.01 – 0.5	0.02 – 1	9 (100%)	24-27, 30-31
PTA	-0.04, 0.24	0.4	Yes	0.1	0.2	-	25
SMA	0.51	0.7	Yes	0.1	0.2	-	25
ZTA	-0.17, -0.05	0.4	Yes	0.1	0.4	200 (100%)	32
Ce ^{4+/3+}	1.48	0	No	0.01 – 0.6	N/A	-	33, 37
V ^{3+/2+}	-0.26	0	No	0.01 – 5	0.01 – 5	120 h @ 110 mA/cm ²	33-36, 38
V ^{5+/4+}	0.99	0	No	0.1 – 1.6	N/A	120 h @ 110 mA/cm ²	34-35
DHPS	-0.05	14.6	Yes	0.005 – 1	0.01 – 2	82 h @ 20 mA/cm ²	41

Information is given based on what was available in the referenced publications. Hydrogen storage density was approximated assuming 100% faradaic efficiency and from the maximum solubility of mediators if stated or commonly known. Cycles are based on demonstrations of decoupled water splitting, not of sole-mediator stability tests.

Table 2. Mass-normalized hydrogen-production rates reported for Type 2 decoupled water-splitting systems and turnover numbers calculated from the reports.

Catalyst	Mediator	H ₂ Rate (mmol hr ⁻¹ mg ⁻¹)	Turnover Number	Ref.
Pt/C (1%)	STA	2861	2,600	24
Pt/C (3%)	STA	423	750	24
Pt/C (5%)	STA	368	530	24
Rh/C (5%)	STA	241	280	24

Pt/C (5%)	STA	47	100	30
Pt/C (20%)	ZTA	121	620	32
Pt/C (1%)	LiPWO	3500	13,600	13
Ni ₅ P ₄ (bulk)	STA	1.198	4.1	25
Mo ₂ C (bulk)	STA	1.006	3.5	25
Mo ₂ C (bulk)	V(II/III)	2.95	155	36
MoS ₂ (bulk)	STA	0.438	2.1	25
Ni ₂ P (bulk)	STA	0.25	2.7	25
Ni ₂ P (1%)	STA	9.418	97	25
Ni ₂ P (1%)	PTA	0.883	7.3	25
CoP	STA	1.92	43	26

H₂ rate data are based on either explicit statement or other available information in the referenced publications. Turnover numbers were calculated based on data and figures for gas evolution found in the original publications which were not originally focused on calculating TON.

Table 3. Properties of mediators used as solids in decoupled water-splitting systems.

Mediator	E^0 (V vs. RHE)	pH	Proton balance	Mediator Density [g/cm ³]	Storage Density [g H ₂ /L]	Stability [Cycles] (Retained Capacity)	Ref.
NiOOH/Ni(OH) ₂	1.36	13.6	Yes	4.1	44.2	100 (100%)	10, 42, 45-46, 58, 60-61
NaTi ₂ (PO ₄) ₃	0.24	13.7	No	2.84	14.1	16 (100%)	46
MnO ₂ /MnOOH	0.98	14.1	Yes	5.03	57.9	3 (96%)	47
MnO ₂ /Mn ²⁺	0.87	0	No	-	-	-	48
FeOx	0.15	13.6	No	-	-	50	49, 97
PTPAn	0.7	0.3	No	-	-	120 (100%)	50
PTO	0.25, 0.48	0.3	Yes	2.11	12.3	300	51
PANI	0.39, 0.85	0.3	Yes	1.36	6.3	40 (92%)	52
Ni-Mn-P/NF	1.3	13.6	Yes	-	-	25	54
Na _{0.44} MnO ₂	0.81, 0.91, 1.13, 1.20, 1.34	13.7	No	-	-	50	56
Ni _{0.9} Co _{0.1} (OH) ₂	1.31-1.41	15	Yes	-	-	100	58

Information is given based on what was available in the referenced publications. Hydrogen storage density was approximated assuming 100% faradaic efficiency and from the density of solid mediators if stated or commonly known. Cycles are based on demonstrations of decoupled water splitting, not of sole-mediator stability tests.

References:

1. *Technology Roadmap - Hydrogen and Fuel Cells*; International Energy Agency: Paris, 2015.
2. Xiang, C.; Papadantonakis, K. M.; Lewis, N. S., Principles and implementations of electrolysis. *Mater. Horiz.* **2016**, *3*, 169-173.
3. McHugh, P. J.; Stergiou, A. D.; Symes, M. D., Decoupled Electrochemical Water Splitting: From Fundamentals to Applications. *Advanced Energy Materials* **2020**, *10* (44).
4. Huang, J.; Wang, Y., Efficient Renewable-to-Hydrogen Conversion via Decoupled Electrochemical Water Splitting. *Cell Reports Physical Science* **2020**, *1* (8).
5. Paul, A.; Symes, M. D., Decoupled electrolysis for water splitting. *Current Opinion in Green and Sustainable Chemistry* **2021**, *29*, 100453.
6. Liu, X.; Chi, J.; Dong, B.; Sun, Y., Recent Progress in Decoupled H₂ and O₂ Production from Electrolytic Water Splitting. *ChemElectroChem* **2019**, *6* (8), 2157-2166.
7. Wallace, A. G.; Symes, M. D., Decoupling Strategies in Electrochemical Water Splitting and Beyond. *Joule* **2018**, *2* (8), 1390-1395.
8. Gentil, S.; Reynard, D.; Girault, H. H., Aqueous organic and redox-mediated redox flow batteries: a review. *Current Opinion in Electrochemistry* **2020**, *21*, 7-13.
9. You, B.; Sun, Y., Innovative Strategies for Electrocatalytic Water Splitting. *Acc Chem Res* **2018**, *51* (7), 1571-1580.
10. Chen, L.; Dong, X.; Wang, Y.; Xia, Y., Separating hydrogen and oxygen evolution in alkaline water electrolysis using nickel hydroxide. *Nat Commun* **2016**, *7*, 11741.
11. Symes, M. D.; Cronin, L., Decoupling hydrogen and oxygen evolution during electrolytic water splitting using an electron-coupled-proton buffer. *Nat Chem* **2013**, *5* (5), 403-9.
12. Wu, W.; Wu, X.-Y.; Wang, S.-S.; Lu, C.-Z., Phosphomolybdic Acid-Bipolar Membrane: An Efficient and Reversible Coupling for Alkaline Water Electrolysis. *ACS Sustainable Chemistry & Engineering* **2020**.
13. Chen, J. J.; Symes, M. D.; Cronin, L., Highly reduced and protonated aqueous solutions of [P₂W₁₈O₆₂]⁶⁻ for on-demand hydrogen generation and energy storage. *Nat Chem* **2018**, *10* (10), 1042-1047.
14. Züttel, A., Materials for hydrogen storage. *Materials Today* **2003**, *6* (9), 24-33.
15. Rausch, B.; Symes, M. D.; Cronin, L., A bio-inspired, small molecule electron-coupled-proton buffer for decoupling the half-reactions of electrolytic water splitting. *J Am Chem Soc* **2013**, *135* (37), 13656-9.
16. Kirkaldy, N.; Chisholm, G.; Chen, J. J.; Cronin, L., A practical, organic-mediated, hybrid electrolyser that decouples hydrogen production at high current densities. *Chem Sci* **2018**, *9* (6), 1621-1626.
17. Bloor, L. G.; Solarska, R.; Bienkowski, K.; Kulesza, P. J.; Augustynski, J.; Symes, M. D.; Cronin, L., Solar-Driven Water Oxidation and Decoupled Hydrogen Production Mediated by an Electron-Coupled-Proton Buffer. *J Am Chem Soc* **2016**, *138* (21), 6707-10.
18. Li, F.; Yu, F.; Du, J.; Wang, Y.; Zhu, Y.; Li, X.; Sun, L., Water Splitting via Decoupled Photocatalytic Water Oxidation and Electrochemical Proton Reduction Mediated by Electron-Coupled-Proton Buffer. *Chem Asian J* **2017**, *12* (20), 2666-2669.
19. Zhao, Y.; Ding, C.; Zhu, J.; Qin, W.; Tao, X.; Fan, F.; Li, R.; Li, C., A Hydrogen Farm Strategy for Scalable Solar Hydrogen Production with Particulate Photocatalysts. *Angew Chem Int Ed Engl* **2020**.

20. Goodwin, S.; Walsh, D. A., Closed Bipolar Electrodes for Spatial Separation of H₂ and O₂ Evolution during Water Electrolysis and the Development of High-Voltage Fuel Cells. *ACS Appl Mater Interfaces* **2017**, *9* (28), 23654-23661.
21. Ma, C.; Pei, S.; You, S., Closed bipolar electrode for decoupled electrochemical water decontamination and hydrogen recovery. *Electrochemistry Communications* **2019**, *109*.
22. You, B.; Liu, X.; Jiang, N.; Sun, Y., A General Strategy for Decoupled Hydrogen Production from Water Splitting by Integrating Oxidative Biomass Valorization. *J Am Chem Soc* **2016**, *138* (41), 13639-13646.
23. Li, W.; Jiang, N.; Hu, B.; Liu, X.; Song, F.; Han, G.; Jordan, T. J.; Hanson, T. B.; Liu, T. L.; Sun, Y., Electrolyzer Design for Flexible Decoupled Water Splitting and Organic Upgrading with Electron Reservoirs. *Chem* **2018**, *4* (3), 637-649.
24. Rausch, B.; Symes, M. D.; Chisholm, G.; Cronin, L., Decoupled catalytic hydrogen evolution from a molecular metal oxide redox mediator in water splitting. *Science* **2014**, *345* (6202), 1326-1330.
25. MacDonald, L.; McGlynn, J. C.; Irvine, N.; Alshibane, I.; Bloor, L. G.; Rausch, B.; Hargreaves, J. S. J.; Cronin, L., Using earth abundant materials for the catalytic evolution of hydrogen from electron-coupled proton buffers. *Sustainable Energy & Fuels* **2017**, *1* (8), 1782-1787.
26. Wu, W.; Wu, X.-Y.; Wang, S.-S.; Lu, C.-Z., Highly efficient hydrogen evolution from water electrolysis using nanocrystalline transition metal phosphide catalysts. *RSC Advances* **2018**, *8* (69), 39291-39295.
27. Chisholm, G.; Cronin, L.; Symes, M. D., Decoupled electrolysis using a silicotungstic acid electron-coupled-proton buffer in a proton exchange membrane cell. *Electrochimica Acta* **2020**, *331* (135255).
28. Carmo, M.; Fritz, D. L.; Mergel, J.; Stolten, D., A comprehensive review on PEM water electrolysis. *International Journal of Hydrogen Energy* **2013**, *38* (12), 4901-4934.
29. Ghassemzadeh, L.; Kreuer, K.-D.; Maier, J.; Müller, K., Chemical Degradation of Nafion Membranes under Mimic Fuel Cell Conditions as Investigated by Solid-State NMR Spectroscopy. *Journal of Physical Chemistry C* **2010**, *114* (34), 14635-14645.
30. Wu, W.; Wu, X.-Y.; Wang, S.-S.; Lu, C.-Z., Catalytic hydrogen evolution and semihydrogenation of organic compounds using silicotungstic acid as an electron-coupled-proton buffer in water-organic solvent mixtures. *Journal of Catalysis* **2019**, *378*, 376-381.
31. Ma, W.; Xie, C.; Wang, X.; Wang, H.; Jiang, X.; Zhang, H.; Guo, X.; Zong, X.; Li, X.; Li, C., High-Performance Solar Redox Flow Battery toward Efficient Overall Splitting of Hydrogen Sulfide. *ACS Energy Letters* **2019**, *5* (2), 597-603.
32. Lei, J.; Yang, J. J.; Liu, T.; Yuan, R. M.; Deng, D. R.; Zheng, M. S.; Chen, J. J.; Cronin, L.; Dong, Q. F., Tuning Redox Active Polyoxometalates for Efficient Electron-Coupled Proton-Buffer-Mediated Water Splitting. *Chemistry* **2019**, *25* (49), 11432-11436.
33. Amstutz, V.; Toghiani, K. E.; Powlesland, F.; Vrubel, H.; Comninellis, C.; Hu, X.; Girault, H. H., Renewable hydrogen generation from a dual-circuit redox flow battery. *Energy Environ. Sci.* **2014**, *7* (7), 2350-2358.
34. Peljo, P.; Vrubel, H.; Amstutz, V.; Pandard, J.; Morgado, J.; Santasalo-Aarnio, A.; Lloyd, D.; Gummy, F.; Dennison, C. R.; Toghiani, K. E.; Girault, H. H., All-vanadium dual circuit redox flow battery for renewable hydrogen generation and desulfurisation. *Green Chemistry* **2016**, *18* (6), 1785-1797.

35. Piwek, J.; Dennison, C. R.; Frackowiak, E.; Girault, H.; Battistel, A., Vanadium-oxygen cell for positive electrolyte discharge in dual-circuit vanadium redox flow battery. *Journal of Power Sources* **2019**, 439.
36. Reynard, D.; Bolik-Coulon, G.; Maye, S.; Girault, H. H., Hydrogen production on demand by redox-mediated electrocatalysis: A kinetic study. *Chemical Engineering Journal* **2021**, 407.
37. Frey, D.; Kim, J.; Dvorkin, Y.; Modestino, M. A., Spatiotemporal Decoupling of Water Electrolysis for Dual-Use Grid Energy Storage and Hydrogen Generation. *Cell Reports Physical Science* **2020**, 1 (10).
38. Ho, A.; Zhou, X.; Han, L.; Sullivan, I.; Karp, C.; Lewis, N. S.; Xiang, C., Decoupling H₂(g) and O₂(g) Production in Water Splitting by a Solar-Driven V^{3+/2+}(aq,H₂SO₄)|KOH(aq) Cell. *ACS Energy Letters* **2019**, 4 (4), 968-976.
39. McCrory, C. C.; Jung, S.; Ferrer, I. M.; Chatman, S. M.; Peters, J. C.; Jaramillo, T. F., Benchmarking hydrogen evolving reaction and oxygen evolving reaction electrocatalysts for solar water splitting devices. *J Am Chem Soc* **2015**, 137 (13), 4347-57.
40. Walter, M. G.; Warren, E. L.; McKone, J. R.; Boettcher, S. W.; Mi, Q.; Santori, E. A.; Lewis, N. S., Solar Water Splitting Cells. *Chem. Rev.* **2010**, 110 (11), 6446-6473.
41. Zhang, F.; Zhang, H.; Salla, M.; Qin, N.; Gao, M.; Ji, Y.; Huang, S.; Wu, S.; Zhang, R.; Lu, Z.; Wang, Q., Decoupled Redox Catalytic Hydrogen Production with a Robust Electrolyte-Borne Electron and Proton Carrier. *J Am Chem Soc* **2021**, 143 (1), 223-231.
42. Landman, A.; Dotan, H.; Shter, G. E.; Wullenkord, M.; Houaijia, A.; Maljus, A.; Grader, G. S.; Rothschild, A., Photoelectrochemical water splitting in separate oxygen and hydrogen cells. *Nat Mater* **2017**, 16 (6), 646-651.
43. Trotochaud, L.; Young, S. L.; Ranney, J. K.; Boettcher, S. W., Nickel-iron oxyhydroxide oxygen-evolution electrocatalysts: the role of intentional and incidental iron incorporation. *J Am Chem Soc* **2014**, 136 (18), 6744-53.
44. Burke, M. S.; Kast, M. G.; Trotochaud, L.; Smith, A. M.; Boettcher, S. W., Cobalt-iron (oxy)hydroxide oxygen evolution electrocatalysts: the role of structure and composition on activity, stability, and mechanism. *J Am Chem Soc* **2015**, 137 (10), 3638-48.
45. Landman, A.; Halabi, R.; Dias, P.; Dotan, H.; Mehlmann, A.; Shter, G. E.; Halabi, M.; Naseraldeem, O.; Mendes, A.; Grader, G. S.; Rothschild, A., Decoupled Photoelectrochemical Water Splitting System for Centralized Hydrogen Production. *Joule* **2020**, 4 (2), 448-471.
46. Guo, M.; Wang, L.; Zhan, J.; Jiao, X.; Chen, D.; Wang, T., A novel design of an electrolyser using a trifunctional (HER/OER/ORR) electrocatalyst for decoupled H₂/O₂ generation and solar to hydrogen conversion. *Journal of Materials Chemistry A* **2020**, 8 (32), 16609-16615.
47. Choi, B.; Panthi, D.; Nakoji, M.; Kabutomori, T.; Tsutsumi, K.; Tsutsumi, A., A novel water-splitting electrochemical cycle for hydrogen production using an intermediate electrode. *Chemical Engineering Science* **2017**, 157, 200-208.
48. Huang, J.; Xie, Y.; Yan, L.; Wang, B.; Kong, T.; Dong, X.; Wang, Y.; Xia, Y., Decoupled amphoteric water electrolysis and its integration with Mn-Zn battery for flexible utilization of renewables. *Energy & Environmental Science* **2021**.
49. Jin, Z.; Li, P.; Xiao, D., A Hydrogen-Evolving Hybrid-Electrolyte Battery with Electrochemical/Photoelectrochemical Charging from Water Oxidation. *ChemSusChem* **2017**, 10 (3), 483-488.

50. Ma, Y.; Dong, X.; Wang, Y.; Xia, Y., Decoupling Hydrogen and Oxygen Production in Acidic Water Electrolysis Using a Polytriphenylamine-Based Battery Electrode. *Angew Chem Int Ed Engl* **2018**, *57* (11), 2904-2908.
51. Ma, Y.; Guo, Z.; Dong, X.; Wang, Y.; Xia, Y., Organic Proton-Buffer Electrode to Separate Hydrogen and Oxygen Evolution in Acid Water Electrolysis. *Angew Chem Int Ed Engl* **2019**, *58* (14), 4622-4626.
52. Wang, J.; Ji, L.; Teng, X.; Liu, Y.; Guo, L.; Chen, Z., Decoupling half-reactions of electrolytic water splitting by integrating a polyaniline electrode. *Journal of Materials Chemistry A* **2019**, *7* (21), 13149-13153.
53. Shabangoli, Y.; Rahmanifar, M. S.; El-Kady, M. F.; Noori, A.; Mousavi, M. F.; Kaner, R. B., An integrated electrochemical device based on earth-abundant metals for both energy storage and conversion. *Energy Storage Materials* **2018**, *11*, 282-293.
54. Liu, Z.; Zhang, G.; Zhang, K.; Lan, H.; Liu, H.; Qu, J., Low electronegativity Mn bulk doping intensifies charge storage of Ni₂P redox shuttle for membrane-free water electrolysis. *Journal of Materials Chemistry A* **2020**, *8* (7), 4073-4082.
55. Simon, P.; Gogotsi, Y., Materials for electrochemical capacitors. *Nature Materials* **2008**, *7* (11), 845-854.
56. Hou, M.; Chen, L.; Guo, Z.; Dong, X.; Wang, Y.; Xia, Y., A clean and membrane-free chlor-alkali process with decoupled Cl₂ and H₂/NaOH production. *Nat Commun* **2018**, *9* (1), 438.
57. Wang, F.; Li, W.; Wang, R.; Guo, T.; Sheng, H.; Fu, H.-C.; Stahl, S. S.; Jin, S., Modular Electrochemical Synthesis Using a Redox Reservoir Paired with Independent Half-Reactions. *Joule* **2021**, *5* (1), 149-165.
58. Dotan, H.; Landman, A.; Sheehan, S. W.; Malviya, K. D.; Shter, G. E.; Grave, D. A.; Arzi, Z.; Yehudai, N.; Halabi, M.; Gal, N.; Hadari, N.; Cohen, C.; Rothschild, A.; Grader, G. S., Decoupled hydrogen and oxygen evolution by a two-step electrochemical–chemical cycle for efficient overall water splitting. *Nature Energy* **2019**, *4* (9), 786-795.
59. H2Pro. <https://www.h2pro.co/>.
60. Landman, A.; Hadash, S.; Shter, G. E.; Dotan, H.; Rothschild, A.; Grader, G., High Performance Core-Shell Ni/Ni(OH)₂ Electrospun Nanofiber Anodes for Decoupled Water Splitting. *ChemRxiv* **2020**.
61. Ma, Y.; Dong, X.; Wang, R.; Bin, D.; Wang, Y.; Xia, Y., Combining water reduction and liquid fuel oxidization by nickel hydroxide for flexible hydrogen production. *Energy Storage Materials* **2018**, *11*, 260-266.
62. Wang, Z.; Li, C.; Domen, K., Recent developments in heterogeneous photocatalysts for solar-driven overall water splitting. *Chem Soc Rev* **2018**.
63. Maeda, K., Z-Scheme Water Splitting Using Two Different Semiconductor Photocatalysts. *ACS Catalysis* **2013**, *3* (7), 1486-1503.
64. Nichols, E. M.; Gallagher, J. J.; Liu, C.; Su, Y.; Resasco, J.; Yu, Y.; Sun, Y.; Yang, P.; Chang, M. C.; Chang, C. J., Hybrid bioinorganic approach to solar-to-chemical conversion. *Proc Natl Acad Sci U S A* **2015**, *112* (37), 11461-6.
65. Belleville, P.; Guillet, F.; Pons, A.; Deseure, J.; Merlin, G.; Druart, F.; Ramousse, J.; Grindler, E., Low voltage water electrolysis: Decoupling hydrogen production using bioelectrochemical system. *International Journal of Hydrogen Energy* **2018**, *43* (32), 14867-14875.

66. Chen, X.; Lobo, F. L.; Bian, Y.; Lu, L.; Chen, X.; Tucker, M. P.; Wang, Y.; Ren, Z. J., Electrical decoupling of microbial electrochemical reactions enables spontaneous H₂ evolution. *Energy & Environmental Science* **2020**, *13* (2), 495-502.
67. Onuki, K.; Kubo, S.; Terada, A.; Sakaba, N.; Hino, R., Thermochemical water-splitting cycle using iodine and sulfur. *Energy & Environmental Science* **2009**, *2* (5).
68. Noh, H.; Kung, C.-W.; Otake, K.-i.; Peters, A. W.; Li, Z.; Liao, Y.; Gong, X.; Farha, O. K.; Hupp, J. T., Redox-Mediator-Assisted Electrocatalytic Hydrogen Evolution from Water by a Molybdenum Sulfide-Functionalized Metal–Organic Framework. *ACS Catalysis* **2018**, *8* (10), 9848-9858.
69. Zong, X.; Han, J.; Seger, B.; Chen, H.; Lu, G. M.; Li, C.; Wang, L., An integrated photoelectrochemical-chemical loop for solar-driven overall splitting of hydrogen sulfide. *Angew Chem Int Ed Engl* **2014**, *53* (17), 4399-403.
70. Du, J.; Lang, Z.-L.; Ma, Y.-Y.; Tan, H.-Q.; Liu, B.-L.; Wang, Y.-H.; Kang, Z.-H.; Li, Y.-G., Polyoxometalate-based electron transfer modulation for efficient electrocatalytic carbon dioxide reduction. *Chemical Science* **2020**, *11* (11), 3007-3015.
71. Huang, J.; Guo, Z.; Dong, X.; Bin, D.; Wang, Y.; Xia, Y., Low-cost and high safe manganese-based aqueous battery for grid energy storage and conversion. *Science Bulletin* **2019**, *64* (23), 1780-1787.
72. Mulder, F. M.; Weninger, B. M. H.; Middelkoop, J.; Ooms, F. G. B.; Schreuders, H., Efficient electricity storage with a battolyser, an integrated Ni–Fe battery and electrolyser. *Energy & Environmental Science* **2017**, *10* (3), 756-764.
73. Weninger, B. M. H.; Mulder, F. M., Renewable Hydrogen and Electricity Dispatch with Multiple Ni-Fe Electrode Storage. *ACS Energy Lett* **2019**, *4* (2), 567-571.
74. Chandesris, M.; Médeau, V.; Guillet, N.; Chelghoum, S.; Thoby, D.; Fouda-Onana, F., Membrane degradation in PEM water electrolyzer: Numerical modeling and experimental evidence of the influence of temperature and current density. *International Journal of Hydrogen Energy* **2015**, *40* (3), 1353-1366.
75. Grigoriev, S. A.; Dzhus, K. A.; Bessarabov, D. G.; Millet, P., Failure of PEM water electrolysis cells: Case study involving anode dissolution and membrane thinning. *International Journal of Hydrogen Energy* **2014**, *39* (35), 20440-20446.
76. Stucki, S.; Scherer, G. G.; Schlagowski, S.; Fischer, E., PEM water electrolyzers: evidence for membrane failure in 100kW demonstration plants. *Journal of Applied Electrochemistry* **1998**, *28*, 1041-1049.
77. Di Profio, P.; Arca, S.; Rossi, F.; Filipponi, M., Comparison of hydrogen hydrates with existing hydrogen storage technologies: Energetic and economic evaluations. *International Journal of Hydrogen Energy* **2009**, *34* (22), 9173-9180.
78. Parks, G.; Boyd, R.; Cornish, J.; Remick, R. *Hydrogen Station Compression, Storage, and Dispensing Technical Status and Costs*; NREL: 2014.
79. Gardiner, M. *DOE Hydrogen and Fuel Cells Program Record: Energy requirements for hydrogen gas compression and liquefaction as related to vehicle storage needs*; 2009.
80. Schalenbach, M.; Carmo, M.; Fritz, D. L.; Mergel, J.; Stolten, D., Pressurized PEM water electrolysis: Efficiency and gas crossover. *International Journal of Hydrogen Energy* **2013**, *38* (35), 14921-14933.
81. Schalenbach, M.; Stolten, D., High-pressure water electrolysis: Electrochemical mitigation of product gas crossover. *Electrochimica Acta* **2015**, *156*, 321-327.

82. Marangio, F.; Santarellia, M.; Pagania, M.; Cali, M., Direct High Pressure Hydrogen Production: a Laboratory Scale PEM Electrolyser Prototype. *ECS Transactions* **2009**, *17*.
83. Bienvenu, G. Method for co-generation of electric energy and hydrogen. US 8,617,766, 2013.
84. Sonnen, D. M.; Reiner, R. S.; Atalla, R. H.; Weinstock, I. A., Degradation of Pulp-Mill Effluent by Oxygen and Na₅[PV₂Mo₁₀O₄₀], a Multipurpose Delignification and Wet Air Oxidation Catalyst. *Industrial & Engineering Chemistry Research* **1997**, *36* (10), 4134-4142.
85. Zeng, K.; Zhang, D., Recent progress in alkaline water electrolysis for hydrogen production and applications. *Progress in Energy and Combustion Science* **2010**, *36* (3), 307-326.
86. Nouri-Khorasani, A.; Tabu Ojong, E.; Smolinka, T.; Wilkinson, D. P., Model of oxygen bubbles and performance impact in the porous transport layer of PEM water electrolysis cells. *International Journal of Hydrogen Energy* **2017**, *42* (48), 28665-28680.
87. Mayyas, A.; Ruth, M.; Pivovar, B.; Bender, G.; Wipke, K. *Manufacturing Cost Analysis for Proton Exchange Membrane Water Electrolyzers*; National Renewable Energy Laboratory: Golden, CO, 2018.
88. Ruth, M.; Mayyas, A.; Mann, M., Manufacturing Competitiveness Analysis for PEM and Alkaline Water Electrolysis Systems. In *Fuel Cell Seminar and Energy Expo*, 2017.
89. Colella, W. G.; James, B. D.; Moton, J. M.; Saur, G.; Ramsden, T., Techno-economic Analysis of PEM Electrolysis for Hydrogen Production. In *Electrolytic Hydrogen Production Workshop*, NREL, Golden, CO, 2014.
90. Bjerketvedt, D.; Mjaavatten, A., A hydrogen-air explosion in a process plant: a case history. In *5th International Conference on Hydrogen Safety*, 2005.
91. Saji, G., Root cause study on hydrogen generation and explosion through radiation-induced electrolysis in the Fukushima Daiichi accident. *Nuclear Engineering and Design* **2016**, *307*, 64-76.
92. DiLisi, G. A., The Hindenburg Disaster: Combining Physics and History in the Laboratory. *The Physics Teacher* **2017**, *55* (5), 268-273.
93. Jerkiewicz, G., Standard and Reversible Hydrogen Electrodes: Theory, Design, Operation, and Applications. *ACS Catalysis* **2020**, 8409-8417.
94. Berger, A.; Segalman, R. A.; Newman, J., Material requirements for membrane separators in a water-splitting photoelectrochemical cell. *Energy Environ. Sci.* **2014**, *7* (4), 1468-1476.
95. Barbir, F., PEM electrolysis for production of hydrogen from renewable energy sources. *Solar Energy* **2005**, *78* (5), 661-669.
96. Onda, K.; Kyakuno, T.; Hattori, K.; Ito, K., Prediction of production power for high-pressure hydrogen by high-pressure water electrolysis. *Journal of Power Sources* **2004**, *132* (1-2), 64-70.
97. Wang, H.; Liang, Y.; Gong, M.; Li, Y.; Chang, W.; Mefford, T.; Zhou, J.; Wang, J.; Regier, T.; Wei, F.; Dai, H., An ultrafast nickel-iron battery from strongly coupled inorganic nanoparticle/nanocarbon hybrid materials. *Nat Commun* **2012**, *3*, 917.